Similar categorical representation from sound and sight in the occipito-temporal cortex of sighted and blind

Authors:

Stefania Mattioni *[1,2], Mohamed Rezk [1,2], Ceren Battal [1,2], Roberto Bottini[1], Karen E. Cuculiza Mendoza [1], Nikolaas N. Oosterhof [1], Olivier Collignon*[1,2]

Affiliations:

[1] Centre for Mind/Brain Studies, University of Trento, Trento, Italy

[2] Institute of research in Psychology (IPSY) & Institute of Neuroscience (IoNS) - University of Louvain (UCLouvain), Louvain, Belgium

* Correspondence should be addressed to: Stefania Mattioni (stefania.mattioni@uclouvain.be) and Olivier Collignon (olivier.collignon@uclouvain.be).

Abstract

The Ventral Occipito-Temporal Cortex (VOTC) shows reliable category selective response to visual information. Do the development, topography and information content of this categorical organization depend on visual input or even visual experience? To further address this question, we used fMRI to characterize the brain responses to eight categories (4 living, 4 non-living) presented acoustically in sighted and early blind individuals, and visually in a separate sighted group. Using a combination of decoding and representational similarity analyses, we observed that VOTC reliably encodes sounds categories in the sighted and blind groups, using a representational structure strikingly similar to the one found in vision. Moreover, we found that the representational connectivity between VOTC and large-scale brain networks was substantially similar across modalities and groups. Blind people however showed higher decoding accuracies and higher inter-subject consistency for the representation of sounds in VOTC, and the correlation between the representational structure of visual and auditory categories was almost double in the blind when compared to the sighted group. Crucially, we also demonstrate that VOTC represents the categorical membership of sounds rather that their acoustic features in both groups. Our results suggest that early visual deprivation triggers an extension of the intrinsic categorical organization of VOTC that is at least partially independent from vision.

Keywords: blindness; category perception; crossmodal plasticity; fMRI; multivariate analyses; auditory; visual.

Introduction

The study of sensory deprived individuals represents a unique model system to test how experience interacts with intrinsic biological constraints to shape the development of the functional organization of the brain. One of the most striking demonstrations of experience-dependent plasticity comes from studies of blind individuals showing that the occipital cortex (traditionally considered as purely visual) massively extends its response to non-visual inputs (Neville & Bavelier, 2002; Sadato et al., 1998).

But what are the mechanisms guiding this brain reorganization process? It was suggested that the occipital cortex of people born blind repurposes its response toward new functions that are distant from the typical tuning of these regions for vision (Bedny, 2017). In fact, the functional organization of occipital regions has been thought to develop based on innate protomaps implementing computational bias for low-level visual features including retinal eccentricity bias (Malach, Levy, & Hasson, 2002), orientation content (Rice, Watson, Hartley, & Andrews, 2014), spatial frequency content (Rajimehr, Devaney, Bilenko, Young, & Tootell, 2011) and the average curvilinearity/rectilinearity of stimuli (Nasr, Echavarria, & Tootell, 2014). This proto-organization would serve as low-level visual biases scaffolding experience-dependent domain specialization (Arcaro & Livingstone, 2017; Gomez, Barnett, & Grill-Spector, 2019). Consequently, in absence of visual experience, the functional organization of the occipital cortex cannot develop according to this proto-organization and those regions may therefore switch their functional tuning toward distant computations (Bedny, 2017).

In striking contrast with this view, several studies suggested that the occipital cortex of congenitally blind people maintains a division of computational labor somewhat similar to the one characterizing the sighted brain (Amedi, Raz, Azulay, Malach, & Zohary, 2010; Dormal & Collignon, 2011; Ricciardi et al., 2007). Perhaps, the most striking demonstration that the occipital cortex of blind people develops a similar coding structure and topography as the one typically observed in sighted

people comes from studies exploring the response properties of the ventral occipito-temporal cortex (VOTC). In sighted individuals, lesion and neuroimaging studies have demonstrated that VOTC shows a medial to lateral segregation in the response to living and non-living visual stimuli, respectively, and that some specific regions respond preferentially to visual objects of specific categories like the fusiform face area (FFA; Kanwisher, McDermott, & Chun, 1997; Tong, Nakayama, Moscovitch, Weinrib, & Kanwisher, 2000), the extrastriate body area (EBA; Downing et al., 2001), the parahippocampal place area (PPA; Epstein & Kanwisher, 1998), and the visual word form area (VWFA; McCandliss, Cohen, & Dehaene, 2003). The medial-to-lateral bias underlying animate–inanimate coding was also found in the VOTC of early blind individuals (Wang et al., 2015). In addition, the functional preference for words (Reich, Szwed, Cohen, & Amedi, 2011) or letters (Striem-Amit, Cohen, Dehaene, & Amedi, 2012), motion (Dormal, Rezk, Yakobov, Lepore, & Collignon, 2016; Poirier, Collignon, Scheiber, & Volder, 2004), places (He et al., 2013; Wolbers, Klatzky, Loomis, Wutte, & Giudice, 2011), bodies (Kitada et al., 2014; Striem-Amit & Amedi, 2014), tools (Peelen et al., 2013) and shapes (Amedi et al., 2007) in early blind partially overlaps with similar categorical responses in sighted people when processing visual inputs.

Distributed multivariate pattern analyses (Haxby et al., 2001) have also supported the idea that the large-scale categorical layout in VOTC share similarities between sighted and blind people (Handjaras et al., 2016; Hurk, Baelen, Op, & Beeck, 2017; Peelen, He, Han, Caramazza, & Bi, 2014; Wang et al., 2015). For example, it was shown that the tactile exploration of different manufactured objects (shoes and bottles) elicits distributed activity in VOTC of blind people somehow similar to the one observed in sighted people in vision (Pietrini et al., 2004). A recent study demonstrated that the response patterns elicited by sounds of four different categories in the VOTC of blind people could successfully predict the categorical response to images of the same categories in the VOTC of sighted controls, suggesting overlapping distributed categorical response in sighted for vision and in blind for sounds (Hurk et al., 2017). All together, these studies suggest that there is more to the development of the categorical response of VOTC than meets the eye

(Collignon, Dormal, & Lepore, 2012).

However, these researches leave several important questions unanswered. If a spatial overlap exists between the sighted processing visual inputs and the blind processing non-visual material, whether VOTC represents similar informational content in both groups remains unknown (Hurk et al., 2017). It is, for instance, possible that the overlap in categorical responses between groups comes from the fact that VOTC represents visual attributes in the sighted (Arcaro & Livingstone, 2017; Gomez et al., 2019) and acoustic attributes in the blind due to crossmodal plasticity (Bavelier & Neville, 2002). Indeed, several studies involving congenitally blind have shown that their occipital cortex may represent acoustic features – for instance frequencies (Huber, Jiang, & Fine, 2019; Watkins et al., 2013) - at the basis of the development of categorical selectivity in the auditory cortex (Moerel, De Martino, & Formisano, 2012). Such preferential responses for visual or acoustic features in the sighted and blind, respectively, may lead to overlapping patterns of activity for similar categories while implementing separate computations on the sensory inputs. Alternatively, it is possible that the VOTC of both groups code for higher-order categorical membership of stimuli presented in vision in sighted and audition in the blind, at least in partial independence from low-level features of the stimuli.

Another unresolved but important question is whether sighted people also show categorical responses in VOTC to acoustic information similar to the one they show in vision. For instance, the two multivariate studies using sensory (not word) stimulation (tactile, Pietrini et al., 2004; auditory, Hurk et al., 2017) of various categories in sighted and blind either did not find the existence of category-related patterns of response in the ventral temporal cortex of sighted people (Pietrini et al., 2004) or did not report overlapping distributed response between categories presented acoustically or visually in sighted people (Hurk et al., 2017). Therefore, it remains controversial whether similar categorical responses in VOTC for visual and non-visual sensory stimuli only emerge in the absence of bottom-up visual inputs during development or whether it is an organizational property also endowed in the VOTC of sighted people.

Finally, it has been suggested that VOTC regions might display similar functional profile for sound and sight in sighted and blind because different portions of this region integrate specific large-scale brain network sharing similar functional coding. However, empirical evidences supporting this mechanistic account remain scarce.

With these unsolved questions in mind, we relied on a series of complementary multivariate analyses in order to carry out a comprehensive mapping of the representational geometry underlying low-level (acoustic or visual features mapping) and categorical responses to images and sounds in the VOTC of sighted and early blind people. Our results demonstrate that (1) VOTC shows categorical responses to sounds in the sighted and the blind in a representational format highly similar to the one elicited by images of the same categories in sighted people; (2) VOTC shows similar large-scale representational connectivity profiles when processing images in sighted and sounds in sighted and blind people; (3) that blind people however show higher decoding accuracies and higher inter-subject consistency in the representation of auditory categories, and that the correlation between the representational structure of visual and auditory categories is almost double in the blind (r=.66) when compared to the sighted (r=.35) group; (4) that the categorical responses to sounds observed in the VOTC of blind and sighted people abstract from their acoustic features and therefore reflect categorical membership of the sounds. All together these results demonstrate that early visual deprivation triggers an extension of the intrinsic, partially non-visual, categorical organization of VOTC and support a mechanistic account based on the shared representational profile between VOTC and large-scale brain networks.

Materials and methods

Participants

Thirty-four participants completed the auditory version of the fMRI study: 17 early blinds (EBa; 10F) and 17 sighted controls (SCa; 6F). An additional group of 16 sighted participants (SCv; 8F) performed the visual version of the fMRI experiment.

All the blind participants lost sight at birth or before 4 years of age and all of them reported not having visual memories and never used vision functionally (see SI table 1). The three groups were age (range 20-67 years, mean ± SD: 33.29 ± 10.24 for EBa subjects, respectively 23-63, 34.12 ± 8.69 for SCa subjects, and 23-51, 30.88 ± 7.24 for SCv subjects) and gender (χ^2 (2,50) =1.92, p=0.38) matched. One blind subject performed only 2 out of the 5 runs in the fMRI due to claustrophobia; because of that we excluded her data. All subjects were blindfolded during the auditory task. Participants received a monetary compensation for their participation. The ethical committee of the University of Trento approved this study (protocol 2014-007) and participants gave their informed consent before participation.

Stimuli

We decided to use sounds and images, instead of words, because we wanted to access and model the bottom-up cascade of sensory processing starting from the low-level sensory steps until the more conceptual level. This methodological decision was crucial in order to assess what level of sound representation is implemented in VOTC of blind and sighted individuals.

A preliminary experiment was implemented in order to select the auditory stimuli (see SI – Stimuli selection for further details). The final acoustic stimuli set included 24 sounds from 8 different categories (human vocalization, human non-vocalization, birds, mammals, tools, graspable objects, environmental scenes, big mechanical objects) that could be reduced to 4 superordinate categories (human, animals, manipulable objects, big objects/places) (see SI Table 2).

We created a visual version of the stimuli set. The images for the visual experiment were coloured pictures collected from Internet and edited using *GIMP* (https://www.gimp.org). Images were placed on a grey (129 RGB) 400 x 400 pixels background.

Procedure

The experimental session was divided into two parts: first the subjects underwent the fMRI experiment and then they performed a behavioural rating judgment task on the same stimuli used in the fMRI experiment.

Similarity Rating

The behavioural experiment aimed to create individual behavioural dissimilarity matrices to understand how the participants perceived the similarity of our stimuli space. Due to practical constraints, only a subset of our participants underwent the behavioural experiment (15 EBa, 11 SCa, and 9 SCv). We created each possible pair from the 24 stimuli set leading to a total of 276 pairs of stimuli. In the auditory experiment, participants heard each sound of a pair sequentially and were asked to judge from 1 to 7 how similar the two stimuli producing these sounds were. In the visual experiment, we presented each pair of stimuli on a screen to the participants and we asked them to judge from 1 to 7 how similar the two stimuli were. Since their rating was strongly based on the categorical features of the stimuli, we used the data from the behavioural experiment to build the categorical models for the representational similarity analysis (see the section "*Representational similarity analysis: correlation with representational low-level/behavioural models "*).

fMRI experiment

Each participant took part in only one experiment, either in the auditory or in the visual version. We decided to include two separate groups of sighted people, one for each modality, for two crucial reasons. First, we wanted to limit as much as possible the possibility of triggering mental imagery from one modality to the other. Second, since cross-group comparisons of representational dissimilarity analyses represent a core component of our analysis stream, we wanted to ensure a cross-group variance comparable between the blind versus the sighted and the sighted in audition versus the sighted in vision.

The procedure for the two experiments was highly similar (Fig. 1A).

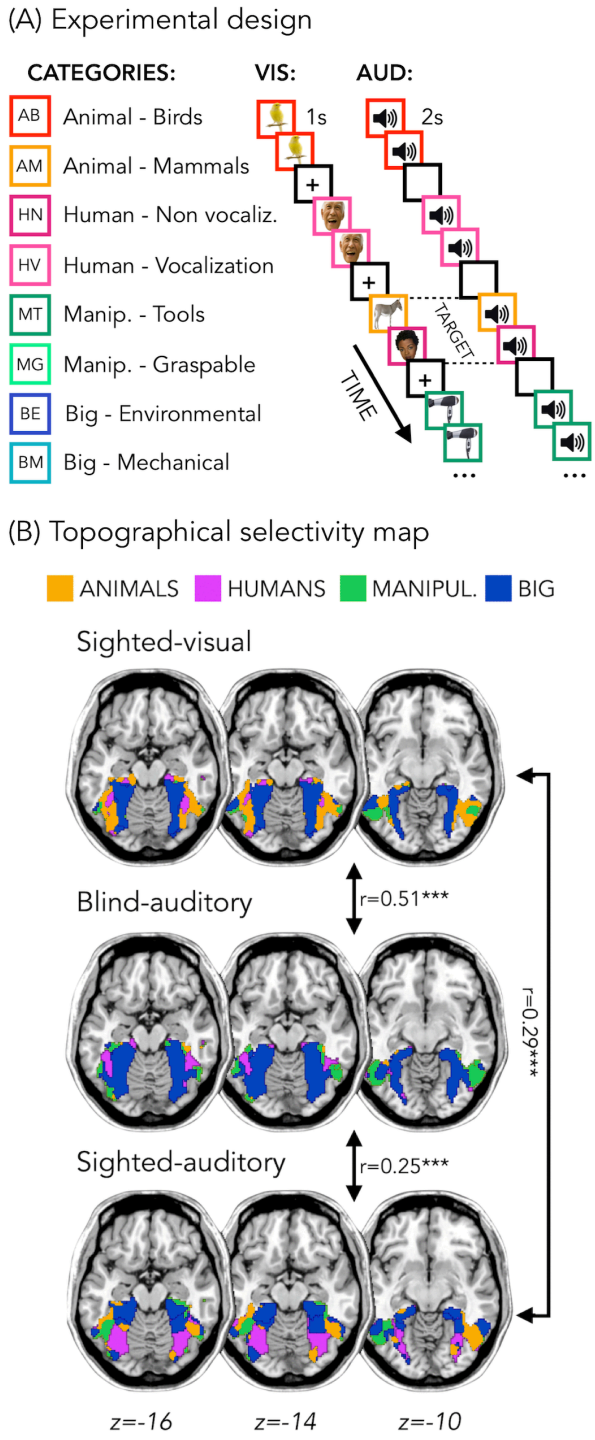

Fig. 1. (A) Categories of stimuli and design of the visual (VIS) and auditory (AUD) fMRI experiments. (B) The untresholded topographical selectivity maps for the sighted-visual (top), the blind-auditory (centre) and the sighted-auditory (bottom) participants. These maps visualize the functional topography of VOTC to the main four categories. We decided to represent maps including the 4 main categories (instead of 8) to simplify visualization of the main effects (the correlation values are almost identical with 8 categories and those maps can be found in supplemental material). The average visual map was correlated with the average auditory map of the blind group (r = 0.51) and of the sighted group (r = 0.29). The averaged auditory map of the blind grou was also correlated with the averaged auditory map of the sighted group (r=0.25).

Before entering the scanner, all the stimuli (either auditory or visual) were presented to each participant to ensure perfect recognition. In the fMRI experiment each trial consisted of the same stimulus repeated twice. Rarely (8% of the occurrences), a trial was made up of two different consecutive stimuli (catch trials). Only in this case participants were asked to press a key with the right index finger if

the second stimulus belonged to the living category and with their right middle finger if the second stimulus belonged to the non-living category. This procedure ensured that the participants attended and processed the stimuli. In the auditory experiment, each pair of stimuli lasted 4s (2s per stimulus) and the inter-stimulus interval between one pair and the next was 2s long for a total of 6s for each trial (Fig. 1A). In the visual experiment, each pair of stimuli lasted 2s (1s per stimulus) and the inter-stimulus interval between one pair and the next was 2s long for a total of 4s for each trial (Fig. 1A).

The use of a ''quick'' event-related fMRI paradigm balances the need for separable hemodynamic responses and the need for presenting many stimuli in the limited time-span of the fMRI experiment. Within both the auditory and the visual fMRI sessions, participants underwent 5 runs. Each run contained 3 repetitions of each of the 24 stimuli, 8 catch trials and two 20s-long rest periods (one in the middle and another at the end of the run). The total duration of each run was 8min and 40s for the auditory experiment and 6min for the visual experiment. For each run, the presentation of trials was pseudo-randomized: two stimuli from the same category were never presented in subsequent trials. The stimuli delivery was controlled using the Psychophysics toolbox implemented in Matlab R2012a (The MathWorks).

fMRI data acquisition and analyses

fMRI data acquisition and preprocessing

We acquired our data on a 4T Bruker Biospin MedSpec equipped with an eight-channel birdcage head coil. Functional images were acquired with a T2*-weighted gradient-recalled echo-planar imaging (EPI) sequence (TR, 2000 ms; TE, 28 ms; flip angle, 73°; resolution, 3x3 mm^3; 30 transverses slices in interleaved ascending order; 3 mm slice thickness; field of view (FoV) 192x192 mm^2). The four initial scans were discarded for steady-state magnetization. Before each EPI run, we performed an additional scan to measure the point-spread function (PSF) of the acquired sequence, including fat saturation, which served for distortion correction that is expected with high-field imaging.

A structural T1-weighted 3D magnetization prepared rapid gradient echo sequence was also acquired for each subject (MP-RAGE; voxel size 1x1x1 mm^3; GRAPPA acquisition with an acceleration factor of 2; TR 2700 ms; TE 4,18 ms; TI (inversion time) 1020 ms; FoV 256 mm; 176 slices).

To correct for distortions in geometry and intensity in the EPI images, we applied distortion correction on the basis of the PSF data acquired before the EPI scans (Zeng & Constable, 2002). Raw functional images were pre-processed and analyzed with SPM8 (Welcome Trust Centre for Neuroimaging London, UK (https://www.fil.ion.ucl.ac.uk/spm/software/spm8/) implemented in MATLAB R2013b (MathWorks). Pre-processing included slice-timing correction using the middle slice as reference, the application of temporally high-pass filtered at 128 Hz and motion correction.

Regions of interest

The anatomical scan was used to segment the brain in separate regions according to the Desikan-Killiany atlas (Desikan et al., 2006) implemented in FreeSurfer (http://surfer.nmr.mgh.harvard.edu).

Six ROIs were selected in each hemisphere: Pericalcarine, Cuneus and Lingual areas were combined to define the early visual cortex (EVC) ROI; Fusiform, Parahippocampal and Infero-Temporal areas were combined to define the ventral occipito-temporal (VOTC) ROI. Then, we combined these areas in order to obtain one bilateral EVC ROI and one bilateral VOTC ROI (Fig. 2A). Our strategy to work on a limited number of relatively large brain parcels has the advantage to minimize unstable decoding results collected from small regions (Norman, Polyn, Detre, & Haxby, 2006) and reduce multiple comparison problems intrinsic to neuroimaging studies (Etzel, Zacks, & Braver, 2013). All analyses, except for the topographical selectivity map (see below), were carried out in subject space for enhanced anatomico-functional precision and to avoid spatial normalization across subjects.

General linear model

The pre-processed images for each participant were analyzed using a general linear model (GLM). For each of the 5 runs, we included 32 regressors: 24 regressors of interest (each stimulus), 1 regressor of no-interest for the target stimulus, 6 head-motion regressors of no-interest and 1 constant. From the GLM analysis we obtained a β-image for each stimulus (i.e. 24 sounds) in each run, for a total of 120 (24 stimuli x 5 runs) beta maps.

Topographical selectivity map

For this analysis, we needed all participants to be coregistered and normalized in a common volumetric space. To achieve maximal accuracy, we relied on the DARTEL (Diffeomorphic Anatomical Registration Through Exponentiated Lie Algebra (Ashburner, 2007) toolbox. DARTEL normalization takes the grey and white matter templates from each subject to create an averaged template based on our own sample that will be used for the normalization. The creation of a study-specific template using DARTEL was performed to reduce deformation errors that are more likely to arise when registering single subject images to an unusually shaped template (Ashburner, 2007). This is particularly relevant when comparing blind and sighted subjects given that blindness is associated with significant changes in the structure of the brain itself, particularly within the occipital cortex (Dormal et al., 2016; Jiang et al., 2009; Pan et al., 2007; Park et al., 2009).

To create the topographical selectivity map (Fig. 1B) we first averaged the β-values among participants of the same group in each voxel inside the VOTC mask for each of our 4 main conditions (animals, humans, manipulable objects and places) separately and we assigned to each voxel the condition producing the highest β-value (winner take all approach). This analysis resulted in specific clusters of voxels that spatially distinguish themselves from their surround in terms of selectivity for a particular condition (Hurk et al., 2017). Finally, to compare how similar are the topographical selectivity maps in the 3 groups we computed the Pearson's correlation between the maps of the different groups. The statistical significance

(against 0) of these correlations was determined using permutation test (100000 iterations), building a null distribution for these correlation values by randomly shuffling the labels of the voxels in VOTC. All the p-values are reported after false discovery rate (FDR) correction implemented using the matlab function *'mafdr'*. We run this analysis using the four (Fig. 1B) and the eight categories (see SI-Fig2) and both analyses lead to almost identical results. We decided to represent the data of the four main categories for simpler visualization of the main effect (topographical overlap across modalities and groups).

MVP-classifications: Binary decoding

We performed a binary MVP-classification to look at the ability of each ROI to distinguish between two categories at time. With 8 categories we can have 28 possible pairs, resulting in 28 binary MVP-classification tests in each ROI. Statistical significance of the binary classification was assessed using t-test against the chance level. We, then, averaged the 28 accuracy values of each subject in order to have 1 mean accuracy value for subject. Statistical significance of the averaged binary classification was assessed using parametric statistics: t-test against zero and ANOVA.

Representational similarity analysis (RSA): *Correlation between neural dissimilarity matrices of the 3 groups.*

We further investigated the functional profile of the ROIs using RSA. RSA was performed using CoSMoMVPA toolbox, implemented in Matlab (r2013b; Matworks). The basic concept of RSA is the dissimilarity matrix (DSM). A DSM is a square matrix where the number of columns and rows corresponds to the number of the conditions (8X8 in this experiment) and it is symmetrical about a diagonal of zeros. Each cell contains the dissimilarity index between the two stimuli. We used the binary MVP-classification as dissimilarity index to build neural DSMs (Carlson, Tovar, Alink, & Kriegeskorte, 2013; Radoslaw Martin Cichy & Pantazis, 2017; Radoslaw Martin Cichy et al., 2013; Dobs, Isik, Pantazis, & Kanwisher, 2019; Haxby, Connolly, & Guntupalli, 2014; Haxby et al., 2011; O'Toole, Jiang, Abdi, & Haxby,

2005; Pereira, Mitchell, & Botvinick, 2009; Proklova, Kaiser, & Peelen, 2019) for each group, in order to compare the functional profile of the ROIs between the 3 groups. In this way, we ended up with a DSM for each group for every ROI.

We preferred to use binary MVP-classification as dissimilarity index to build neural DSMs rather than other types of dissimilarity measures (e.g. Pearson correlation, Euclidean distance, Spearman correlation) since two experimental conditions that do not drive a response and therefore have uncorrelated patterns (noise only, $r \approx 0$) appear very dissimilar ($1 - r \approx 1$). When using a decoding approach instead, due to the intrinsic cross-validation steps, we would find that the two conditions that don't drive responses are indistinguishable, despite their substantial correlation distance (Walther et al., 2016) since the noise is independent between the training and testing partitions, therefore cross-validated estimates of the distance do not grow with increasing noise. This was crucial in our study since we are looking at brain activity elicited by sounds in brain regions that are primarily visual (EVC and VOTC), therefore the level of noise is expected to be high, at least in sighted people.

Finally, we computed the Pearson correlation between the neural DSMs to see if, in each ROI, the same categories that are well or poorly distinguished in vision in the sighted are also well or poorly distinguished in audition in the early blind and/or in the sighted (Fig. 3). For each group, the statistical difference from zero was determined using permutation test (10000 iterations), building a null distribution for these correlation values by computing them after randomly shuffling the labels of the 8X8 matrices. Similarly, the statistical difference between groups was assessed using permutation test (10000 iterations) building a null distribution for these correlation values by computing them after randomly shuffling the group labels. All the p-values are reported after false discovery rate (FDR) correction implemented using the matlab function *'mafdr'*.

Representational similarity analysis (RSA): correlation with representational low-level/behavioural models .

We then intended to investigate which features of the visual and auditory stimuli were represented in the different ROIs of sighted and blind subjects. RSA allows the comparisons between the brain DSMs extracted from specific ROIs with external DSMs, based on physical properties of the stimuli or based on behavioural rating of the perceived categorical similarity our stimuli.

Low-level DSM in the auditory experiment: pitch DSM. Pitch corresponds to the perceived frequency content of a stimulus. We selected this specific low-level auditory feature for two reasons. First, previous studies showed that this physical property of the sounds is distinctly represented in the auditory cortex and may create some low-level bias of auditory category selective responses in the temporal cortex (Giordano, McAdams, Zatorre, Kriegeskorte, & Belin, 2013; Leaver & Rauschecker, 2010; M. Moerel et al., 2012). Second, we confirmed with our own SCa group that, among alternative auditory RDMs based on separate acoustic features (e.g. Harmonicity on noise ratio, Spectral centroid), the pitch model correlated most with brain RDM extracted from the temporal cortex providing strong support that this model was maximally efficient in capturing how encoding of sounds based on acoustic features in auditory cortical regions (SI-Fig1).

We computed a pitch value for each of the 24 auditory stimuli, using the Praat software and an autocorrelation method. This method extracts the strongest periodic component of several time windows across the stimulus and averages them to have one mean pitch value for that stimulus. The "pitch floor" determines the size of the time windows over which these values are calculated in Praat. Based on a previous study, we chose a default pitch floor of 60 Hz (Leaver & Rauschecker, 2010). We then averaged the pitch values across stimuli belonging to the same category. Once we obtained one pitch value for each category, we built the DSM computing the absolute value of the pitch difference for each possible pairwise (see figure 5A). The pitch DSM was not positively correlated with the behavioural DSM of neither SCa (r=–0.36, *p=.06)* nor EBa (r= –0.29, *p=0.13*) (Fig. 4A).

Low-level DSM in the visual experiment: Hmax- C1 model. The Hmax model (Serre,

Wolf, Bileschi, Riesenhuber, & Poggio, 2007) reflects the hierarchical organization of the visual cortex (Hubel & Wiesel, 1962) in a series of layers from V1 to infero-temporal (IT) cortex. To build our low-level visual model we used the output from the V1- complex cells layer. The inputs for the model are the grey-value luminance images presented in the sighted group doing the visual experiment. Each image is first analysed by an array of simple cells (S1) units at 4 different orientations and 16 scales. At the next C1 layer, the image is subsampled through a local Max pooling operation over a neighbourhood of S1 units in both space and scale, but with the same preferred orientation (Serre et al., 2007). C1 layer stage corresponds to V1 cortical complex cells, which shows some tolerance to shift and size (Serre et al., 2007). The outputs of all complex cells were concatenated into a vector as the V1 representational pattern of each image (Khaligh-Razavi & Kriegeskorte, 2014; Kriegeskorte, Mur, & Bandettini, 2008). We averaged the vectors of images from the same category in order to have 1 vector for each category. We, finally, built the (8X8) DSM computing 1- Pearson's correlation of each pair of vectors. The Hmax-C1 DSM was significantly correlated with the SCv behavioural DSM (r=0.56, *p=0.002*) (Fig. 4A).

Behavioural-categorical DSMs. We used the pairwise similarity judgments from the behavioural experiment to build the semantic DSMs. We computed one matrix for each subject that took part in the behavioural experiment and we averaged all the matrices of the participants from the same group to finally obtain three mean behavioural-categorical DSMs, one for each group (i.e. EBa, SCa, SCv; Fig. 4A). The three behavioural matrices were highly correlated between them (SCv-EBa: r=0.89, p<.001; SCv-SCa: r=0.94, p<.001; EBa-SCa: r=0.85, p<.001) and the similarity judgment was clearly performed on a categorical-membership basis (Fig. 4A).

The last step consisted in comparing neural and external DSMs models using a second order correlation. Because we wanted to investigate each external model independently from the other, we relied on Pearson's linear partial correlation: in the auditory experiment, we removed the influence of the pitch similarity when we were computing the correlation with the behavioural matrix, and vice versa; in the visual

experiment, we removed the influence of the Hmax-C1 model similarity, when we were computing the correlation with the behavioural matrix, and vice versa. In this way, we could measure the partial correlation for each external model for each participant separately (Fig. 4A). Significances within group were determined using one-tailed permutation tests (100000 iterations), building a null distribution for these values by computing them after randomly shuffling the labels of the neural RDMs. Statistical differences between groups were determined using permutation tests (100000 iterations), building a null distribution for these values by computing them after randomly shuffling the groups' labels. All the p-values are reported after false discovery rate (FDR) correction.

RSA: Inter-subjects correlation

To examine the commonalities of the neural representational space across subjects in VOTC, we extracted the neural DSM of every subject individually and then correlated it with the neural DSM of every other subject. Since we have 49 participants in total, this analysis resulted in a 49X49 matrix (Fig. 5), in which each line and column represents the correlation of one subject's DSM with all other subjects' DSM. The three main squares in the diagonal (Fig. 5) represent the within group correlation of the 3 groups. We averaged the value within each main square on the diagonal to obtain a mean value of within group correlation for each group. The three main off diagonal squares (Fig. 5) represent the between groups correlation of the 3 possible groups' pairs (i.e. 1.SCv/EBa; 2.SCv-SCa; 3.EBa-SCa). We averaged the value within each main off-diagonal square in order to obtain a mean value of between groups correlation for each groups' pair.

The significance of the within- and between-groups correlations were determined using permutation tests (100.000 iterations), building a null distribution for these values by computing them after randomly shuffling the labels of the RDMs conditions. Similarly, the statistical difference between groups and groups' pairs was assessed using permutation test (10000 iterations) building a null distribution for these correlation values by computing them after randomly shuffling the group labels. The p-values are reported after false discovery rate (FDR) correction.

Representational connectivity analysis

Representational connectivity analysis were implemented to identify the representational relationship among the ROIs composing VOTC and the rest of the brain (Kriegeskorte, Mur, & Bandettini, 2008; Pillet, Beeck, & Masson, 2018). This approach can be considered a type of connectivity where similar RDMs of two ROIs indicate shared representational structure and therefore is supposed to be a proxy for information exchange (Kriegeskorte, Mur, Ruff, et al., 2008). Representational connectivity between two ROIs does not imply a direct structural connection but can provide connectivity information from a functional perspective, assessing to what extent two regions represent information similarly (Xue, Weng, He, & Li, 2013).

To perform this analysis, we included 30 bilateral parcels (covering almost the entire cortex) extracted from the segmentation of individual anatomical scan following the Desikan-Killiany atlas implemented in FreeSurfer (http://surfer.nmr.mgh.harvard.edu). We only excluded 3 parcels (Entorhinal cortex, Temporal Pole and Frontal Pole) because their size was too small and signal too noisy (these regions are notably highly susceptible to signal drop in EPI acquisition) to allowed the extraction of reliable dissimilarity matrices in most of the participants. We merged together the left and right corresponding parcels in order to have a total of 30 bilateral ROIs for each subject. From each ROI we extracted the dissimilarity matrix based on binary decoding accuracies as described in the section "*Representational similarity analysis (RSA)*: *Correlation between neural dissimilarity matrices of the 3 groups"*. Finally, we computed the Pearson's correlation between the 3 seed ROIs (i.e. fusiform gyrus, parahippocampal gyrus and infero-temporal cortex) and all the other 27 ROIs. We ended up with a connectivity profile of 3X27 correlation values for each subject. Then we averaged these values across subjects from the same group in order to have one averaged connectivity profile for each group (Fig. 6). To assess how similar is the connectivity profile of VOTC in the 3 groups, the last step was to compute the Pearson's correlation between the VOTC connectivity profiles of the 3 groups (Fig. 6).

Results

Behavioural ratings

We asked our participants to rate each possible pair of stimuli in the experiment they took part in (either visual or acoustic) and we built three dissimilarity matrices based on their judgments. A visual exploration of the ratings using the dissimilarity matrix visualization revealed a clustering of the stimuli into a main living/non-living distinction, with some sub-clustering such as humans, animals and objects (Fig. 4A). The three DSMs were highly correlated (SCa/EBa: r= .85, *p<0.001*; SCa/SCv: r= .95, *p<0.001*; EBa/SCv: r= .89, *p<0.001*), revealing a similar way to group the stimuli across the three groups following mostly a categorical strategy to classify the stimuli. Based on this observation, we used the behavioural matrices as a categorical/high-level model to contrast with the low-level models built on the physical properties of the stimuli (HmaxC1 and pitch models, Fig. 4A).

Topographical selectivity map

Fig. 1B represents the topographical selectivity maps, which show the voxel-wise preferred stimulus condition based on a winner take-all approach (for the four main categories: animals, humans, small objects & places). In the visual modality, we found the well-known functional selectivity map for visual categories (Julian, Fedorenko, Webster, & Kanwisher, 2012; Kanwisher, 2010). The auditory selectivity maps of the blind subjects closely matched the visual map obtained in sighted controls during vision (r=0.51, p<0.001). This similarity is mostly driven by place-, object- and human-selective clusters bilaterally. The blind map and the visual control map are strongly correlated.

In addition, a similar selectivity map was also observed in the sighted controls using sounds. The correlation was significant both with visual map in sighted (r=.29, p<0.001), and with the auditory map in blinds (r=.25, p<0.001). This correlation was mostly explained by the more anterior part of the place-selective clusters bilaterally, the animal-selective patch bilaterally and the object-selective patch in the left hemisphere.

Here, we report the results on the four main categories for the simplicity of visualization, however in the supplemental material we show that the results including eight categories are almost identical (SI-Fig. 2).

Binary MVP classification

Fig. 2B represents the results from the average binary classification analyses for each group and every ROI (FDR corrected). In SCv and in EBa the averaged decoding accuracy was significantly higher than chance level in both EVC (SCv: DA=69%; $t_{(15)}$=6.69, *p<.00001*; EBa: DA=55%; $t_{(15)}$=4.48, p=*0.0006*) and VOTC (SCv: DA=71%; $t_{(15)}$=7.37, *p<.00001*; EBa: DA=57%; $t_{(15)}$=8.00, p<*0.0001*). In the SCa the averaged decoding accuracy was significantly higher than the chance level in VOTC (DA=54%; $t_{(16)}$=4.32, p=*0.0006*) but not in EVC (DA=51%; $t_{(16)}$=1.70, p=*0.11*). Moreover, independent sample t-tests revealed higher decoding accuracy values in EBa when compared to SCa in both EVC ($t_{(31)}$=2.52, p=*0.017*) and VOTC ($t_{(31)}$=2.08, p=*0.046*).

Results from each binary classification analysis (n=28) for each group are represented in figure 3 panel A1 for EVC and in panel B1 for VOTC. The p-values for each t-test is reported in the SI-table 3.

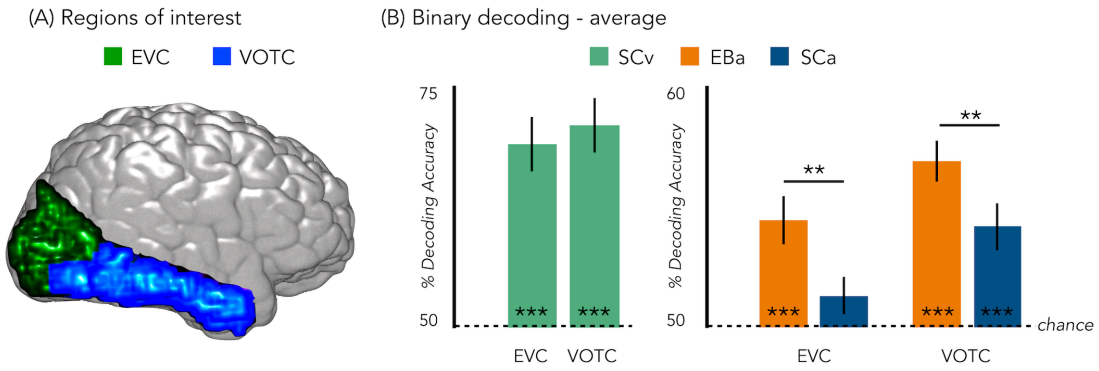

Fig. 2. (A) Representation of the 2 ROIs in one representative subject's brain; (B) Binary decoding averaged results in early visual cortex (EVC) and ventral occipito-temporal cortex (VOTC) for visual stimuli in sighted (green), auditory stimuli in blind (orange) and auditory stimuli in sighted (blue). ***p<.001, **p<.05.

RSA: Correlation between the neural dissimilarity matrices of the 3 groups.

We used the accuracy values from the binary classifications to build neural dissimilarity matrices for each subject in EVC (Fig. 3 - Panel A2) and in VOTC (Fig. 3 - Panel B2). Then, in every ROI we averaged the neural DSMs across subjects from the same group and we computed the correlations (FDR corrected) between averaged DSMs for each groups' pair (i.e. SCv-EBa; SCv-SCa; EBa-SCa).

In EVC, the one-tailed permutation test revealed a significant positive correlation only between the SCv and the EBa DSMs (r=.41; *p=0.03*), whereas the correlation between the SCv and SCa DSMs (r= –.50; *p=0.99*) and the correlation between the SCa and the EBa DSMs (r= –.12; *p=0.88*) were not significant. Moreover, the correlation between SCv and EBa was significantly higher compared to both the correlation between SCv and SCa (corr. diff= .91; *p=0.005*) and the correlation between SCa and EBa (corr. diff= .53; *p=0.04*).

In VOTC, we observed a significant correlation for all the groups' pairs: SCv and EBa (r=.66; *p=0.01*), SCv and SCa (r= .35; *p=0.05*), SCa and EBa (r=.43; *p=0.03*). However, the correlation between SCv and EBa was significantly higher compared to both the correlation between SCv and SCa (corr. diff= .31; *p=0.02*) and the correlation between SCa and EBa (corr. diff= .23; *p=0.03*).

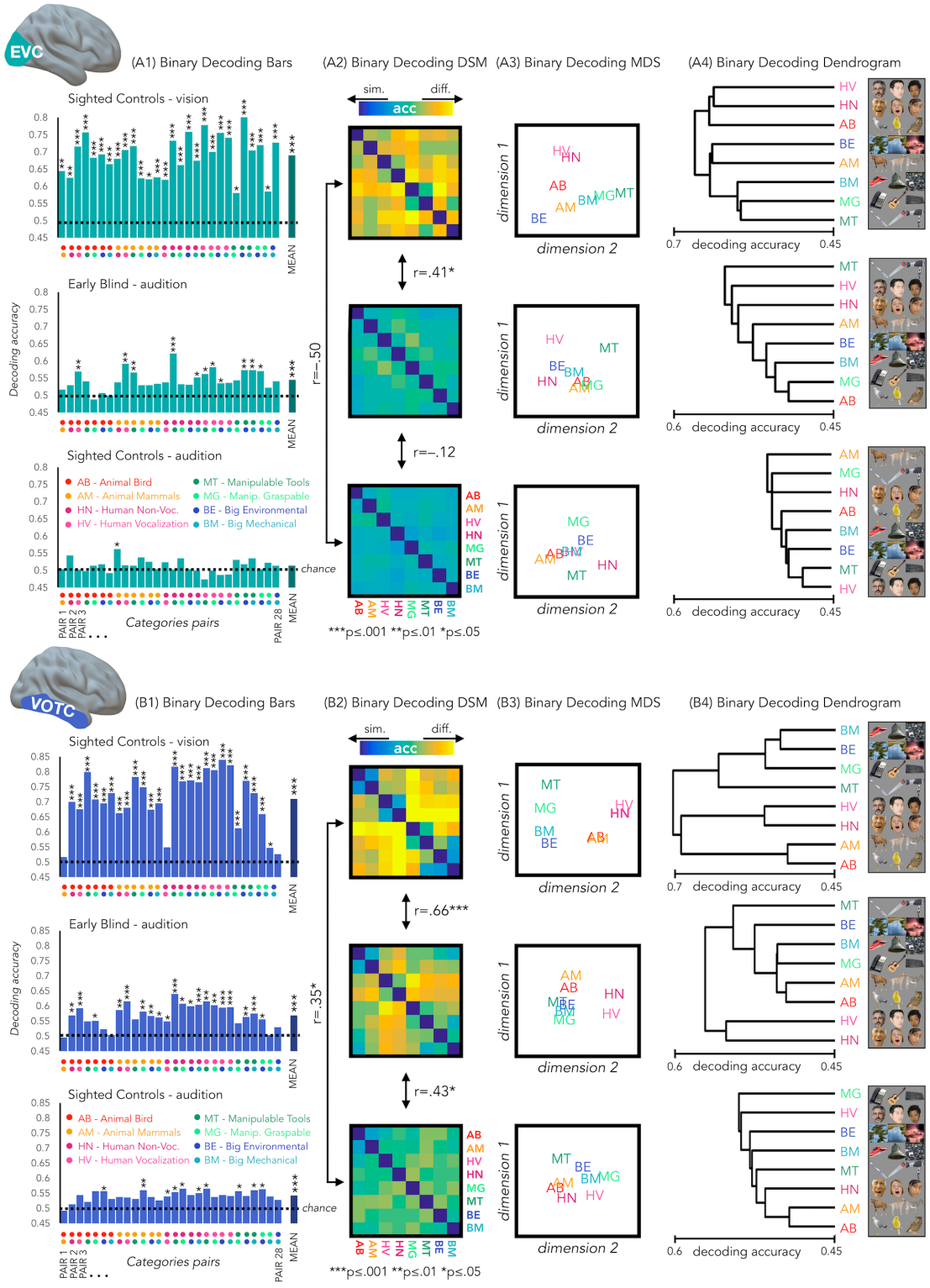

Fig. 3. EVC and VOTC functional profiles. (A1 & B1) Binary decoding bar plots. For each group (SCv: top; EBa: centre; SCa: bottom) the decoding accuracy from the 28 binary decoding analyses are represented. Each column represents the decoding accuracy value coming from the classification analysis between 2 categories. The 2 dots under each column represent the 2 categories. (A2 & B2) The 28 decoding accuracy values are represented in the form of a dissimilarity matrix. Each column and each row of the matrix represent one category. In each square there is the accuracy value coming from

the classification analysis of 2 categories. Blue colors mean low decoding accuracy values and yellow colors mean high decoding accuracy values. (A3 & B3) Binary decoding multidimensional scaling (MDS). The categories have been arranged such that their pairwise distances approximately reflect response pattern similarities (dissimilarity measure: accuracy values). Categories placed close together were based on low decoding accuracy values (similar response patterns). Categories arranged far apart generated high decoding accuracy values (different response patterns). The arrangement is unsupervised: it does not presuppose any categorical structure (Kriegeskorte et al., 2008). (A4 & B4) Binary decoding dendrogram. We performed hierarchical cluster analysis (based on the accuracy values) to assess if EVC(A4) and VOTC (B4) response patterns form clusters corresponding to natural categories in the 3 groups (SCv: top; EBa: centre; SCa: bottom).

RSA: correlation with representational low-level/behavioural models

In order to better understand the representational content of VOTC and EVC, we computed second-order partial correlations between each ROI's DSM and our representational models (i.e. behavioural and low-level DSMs) for each participant. Fig. 4B represents the results (FDR corrected) for the correlation between the brain DSMs in the 3 groups and the representational low-level/behavioural models DSMs (i.e. behavioural, pitch and Hmax-C1 DSMs).

The permutation test revealed that in SCv the EVC's DSM was significantly correlated with both the behavioural DSMs (r=.09; *p=0.01*) and the Hmax-C1 model (r=.14; *p=0.004*). Even though the correlation was numerically higher with the Hmax-C1 model than with the behavioural model, a paired samples t-test did not reveal a significant difference between the two ($t_{(15)=}$0.6, p=.56). The permutation test showed that VOTC's DSM, instead, was significantly correlated with the behavioural model (r=.38, *p<.001*) but not with the Hmax-C1 model (r= –.03, *p=.35*). A paired samples t-test revealed that the difference between the correlation with the two models was significant ($t_{(15)=}$7.93, p<.001).

In the EBa and SCa groups EVC's DSMs were not significantly correlated with neither the behavioural (EBa: r=.04, *p=.22*; SCa: r= –.09, p=.487) nor the pitch model (EBa: r= –.05, *p=.487*; SCa: r= –.08, p=.487). In contrast, the VOTC's DSMs were significantly correlated with the behavioural model both in EBa (r=.14, *p=002*) and in SCa (r=.08, *p=.045*). In addition, a 2 Groups (EBa/SCa) X 2 Models (behavioural/pitch) ANOVA in VOTC revealed a significant main effect of Model

($F_{(31)}$=10.37, *p=.003*), whereas the main effect of Group ($F_{(31)}$=0.006, *p=.94*), and the interaction Group X Model ($F_{(31)}$=3.61, *p=.07*), were both non-significant. A Bonferroni post-hoc test confirmed that the correlation was significantly higher for the behavioural model compared to the pitch model (t=3.22, *p=0.003*) in both groups.

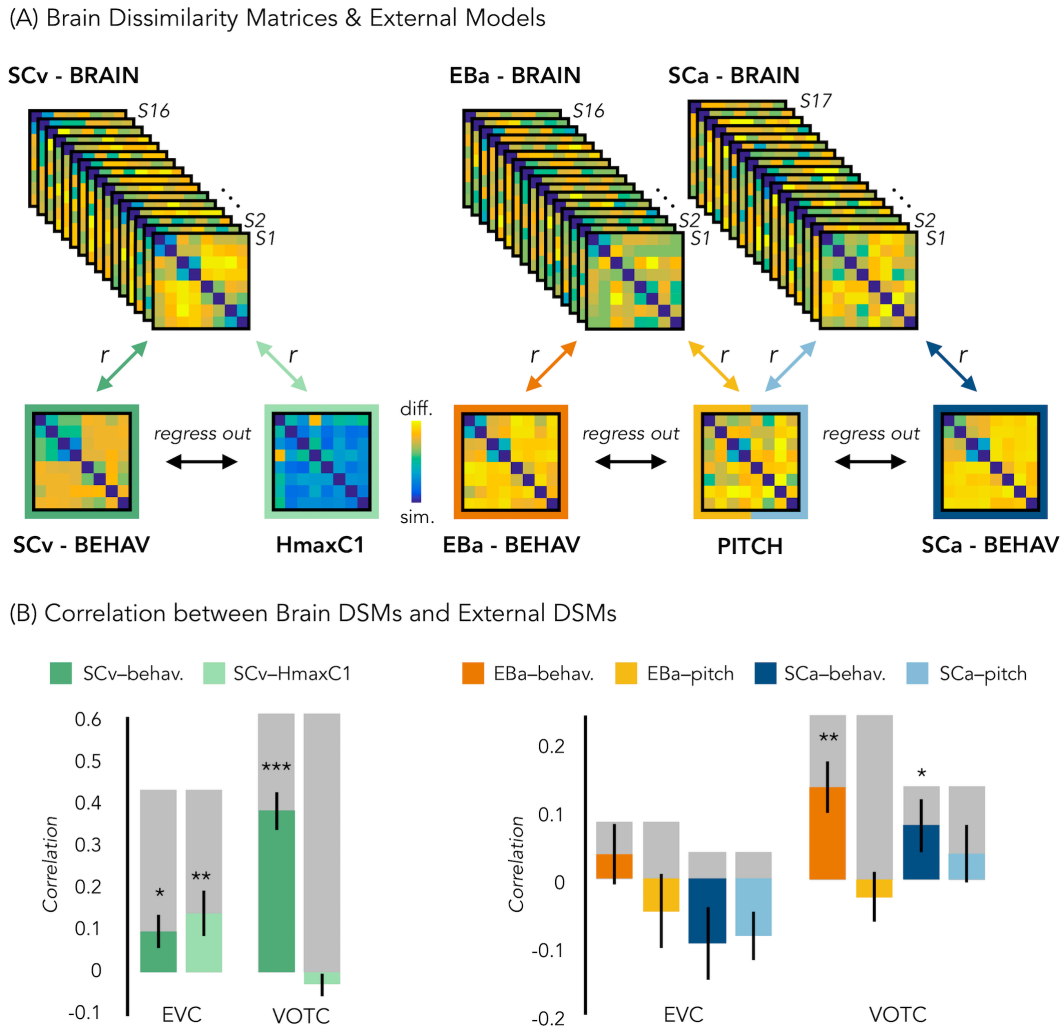

Fig. 4. Representational similarity analysis (RSA) between brain and representational low-level/behavioural models **(A)** In each ROI we computed the brain dissimilarity matrix (DSM) in every subject based on binary decoding of our 8 different categories. In the visual experiment (left) we computed the partial correlation between each subject's brain DSM and the behavioral DSM from the same group (SCv-Behav.) regressing out the shared correlation with the HmaxC1 model, and vice versa. In the auditory experiment (right) we computed the partial correlation between each subject's brain DSM (in both Early Blind and Sighted Controls) and the behavioral DSM from the own group (either EBa-Behav. or SCa-Behav.) regressing out the shared correlation with the pitch model, and vice versa. **(B)** Results from the correlation between representational low-level/behavioural models and

brain DSMs from both EVC and VOTC. On the left are the results from the visual experiment. Dark green: partial correlation between SCv brain DSM and behavioral model; Light green: Partial correlation between SCv brain DSM and HmaxC1 model. On the right are the results from the auditory experiment in both early blind (EBa) and sighted controls (SCa). Orange: partial correlation between EBa brain DSM and behavioral model; Yellow: Partial correlation between EBa brain DSM and pitch model. Dark blue: partial correlation between SCa brain DSM and behavioral model; Light blue: partial correlation between SCa brain DSM and pitch model. For each ROI and group, the grey background bar represents the reliability of the correlational patterns, which provides an approximate upper bound of the observable correlations between representational low-level/behavioural models and neural data (Bracci & Beeck, 2016; Nili et al., 2014). Error bars indicate SEM. ***p<.001, **p<.005, *p<.05. P values are FDR corrected.

RSA: Inter-subjects correlation

We run this analysis to understand how variable was the brain representation in VOTC across subjects belonging either to the same groups or to different groups. Since we have 3 groups, this analysis resulted in 6 different correlation values: 3 values for the 3 within group correlation conditions (SCv; EBa; SCa) and 3 values for the 3 between groups correlation conditions (i.e. SCv-EBa; SCv-SCa; EBa-SCa). Results are represented in figure 5 (FDR corrected).

The permutation test revealed that the correlation between subjects' DSMs in the within group condition was significant in SCv (r=.42; *p<.001*) and EBa (r=.10; *p<.001*), whereas it was not significant in SCa (r=–.03; *p=.98*). Moreover, the correlation between subjects' DSMs was significant in all the three between groups conditions (SCv-EBa: r=.17, *p<.001*; SCv-SCa: r=.04, *p=002*; EBa-SCa: r=.02; *p=.04*). When we ranked the correlations values (Fig. 5) we observed that the highest inter-subject correlation is the within SCv group condition, which was significantly higher compared to all the other five conditions. It was followed by inter-subject correlation between SCv and EBa group and the within EBa group correlation. Interestingly, both the between groups SCv-EBa and the within group EBa correlations were significantly higher compared to the last 3 inter-subjects correlation's values (between SCv-SCa; between EBa-SCa; within SCa).

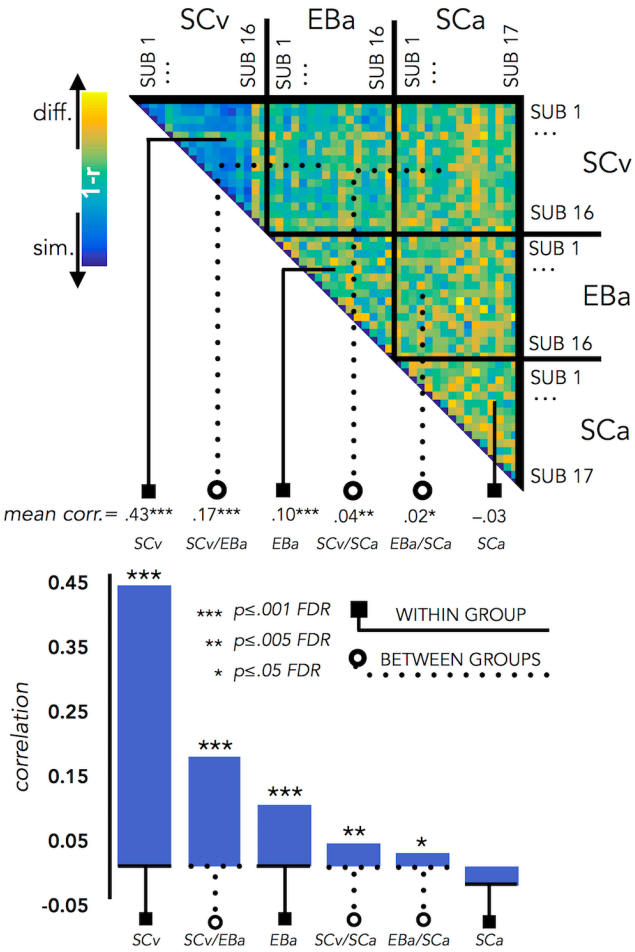

Fig. 5. VOTC Inter-subject correlation within and between groups. Upper panel represents the correlation matrix between the VOTC brain DSM of each subject with all the other subjects (from the same group and from different groups). The mean correlation of each within- and between-group combination is reported in the bottom panel (bar graphs). The straight line ending with a square represents the average of the correlation between subjects from the same group (i.e. within groups conditions: SCv, EBa, SCa), the dotted line ending with the circle represents the average of the correlation between subjects from different groups (i.e. between group conditions: SCv-EBa/ SCv-SCa/ EBa-SCa). The mean correlations are ranked from the higher to the lower inter-subject correlation values.

Representational connectivity analysis

Figure 6 represents the results from the representational connectivity analysis. The representational connectivity profile of VOTC with the rest of the brain is significantly correlated between all pairs of groups (SCv-EBa: r=.48, p<.001; SCv-SCa: r=.40 , p<.001; EBa-SCa: r=.48 ,p<.001; FDR corrected).

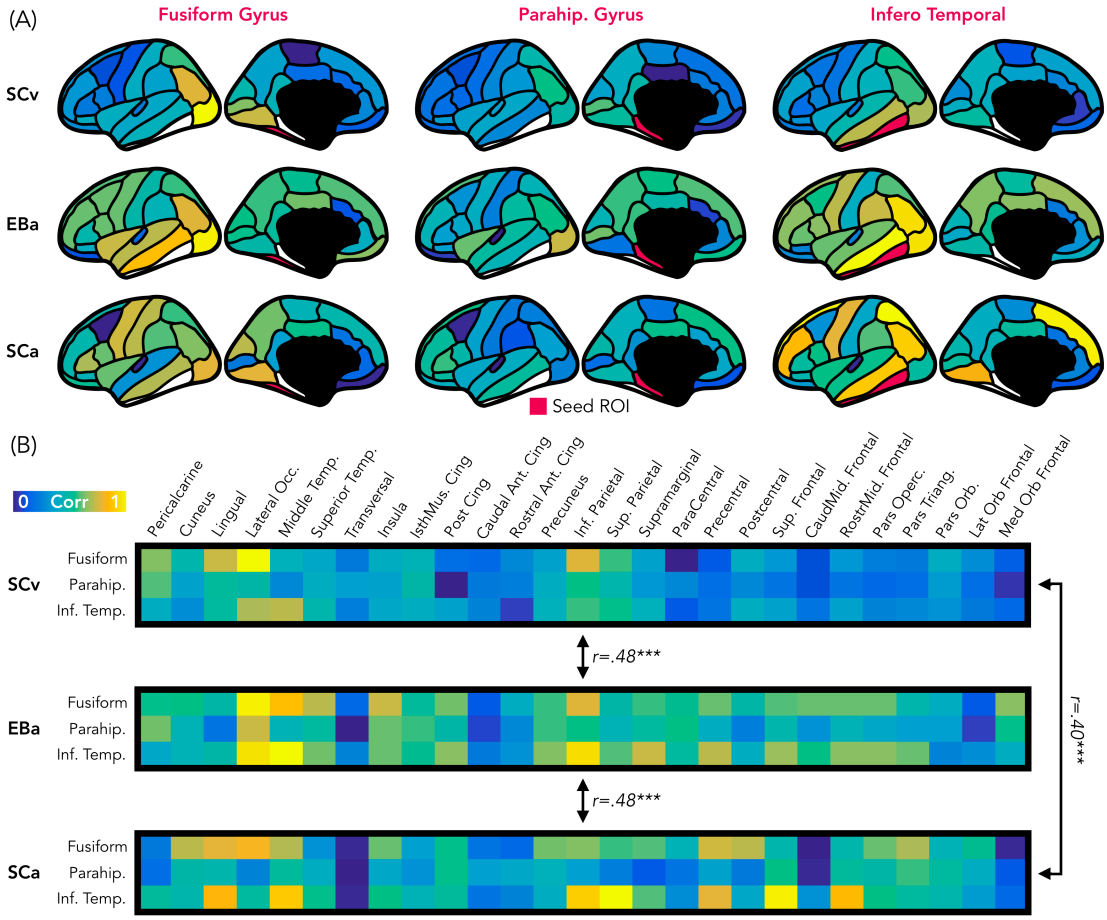

Fig. 6. Representational connectivity. (A) Representation of the z-normalized correlation values between the dissimilarity matrix of the three VOTC seeds (left: Fusiform gyrus, centre: Parahippocampal gyrus, Right: Infero-Temporal cortex) and the dissimilarity matrix of 27 parcels covering the rest of the cortex in the three groups (top: SCv, central: EBa, bottom: SCa). Blue colors represent low correlation with the ROI seed; yellow color represent high correlation with the ROI seed. (B) The z-normalized correlation values are represented in format of one matrix for each group. This connectivity profile is correlated between groups. SCv: sighted control-vision; EBa: early blind-audition; SCa: sighted control-audition.

Discussion

In our study, we demonstrate that VOTC reliably encodes the categorical membership of sounds from eight different categories in sighted and blind people, using a topography (Fig. 1B), representational format (Fig. 3) and a representational connectivity profile (Fig. 6) strikingly similar to the one observed in response to images of similar categories in vision. In contrast to previous studies that have used linguistic stimuli to investigate the pre-existing representation of categories in

VOTC (Borghesani et al., 2016; Martin, Douglas, Newsome, Man, & Barense, 2017; Peelen et al., 2013; Peelen & Downing, 2017; Striem-Amit, Wang, Bi, & Caramazza, 2018; Wang et al., 2015), we employed sensory-related non-linguistic stimuli (sounds), in order to investigate both the sensory (acoustic) and categorical nature of the representation implemented in VOTC. To the limit of our knowledge, only one recent study investigated the macroscopic functional organization of VOTC during categorical processing of auditory and visual stimuli in sighted and in blind individuals (Hurk et al., 2017). They found that it is possible to predict the global large-scale distributed pattern of activity generated by different categories presented visually in sighted using the pattern of activity generated by the same categories presented acoustically in early blind. Relying on a different analytical stream focusing on representational matrices extracted from pairwise decoding of our eight categories, our study support and extend those findings by showing that VOTC reliably encodes sounds categories in blind people using a representational structure strikingly similar to the one found in vision. However, our study goes beyond those previous results in at least four significant ways. First, our study showed that a similar categorical representational structure in VOTC for sounds and images is also observable in sighted people. This result is crucial to support the idea that the intrinsic categorical organization of VOTC might be partially independent from vision even in sighted and, therefore that such intrinsic functional scaffolding may constrain the way crossmodal plasticity expresses in early blind people. Second, we showed that brain regions that represent information similarly (or dissimilarly) compared to VOTC are similar when we present different categories in visual format in sighted and in auditory format in both blind and sighted. This result provides strong support to the general hypothesis that the functional tuning of a region is determined by large-scale connectivity patterns with regions involved in similar coding strategies (Behrens & Sporns, 2012; Mahon & Caramazza, 2011; Passingham, Stephan, & Kötter, 2002). Third, our design allowed us to investigate which dimension of sound features, either categorical membership or acoustic properties, may determine the response properties of VOTC. By harnessing the opportunities provided by representational similarity analyses, we demonstrate that categorical

membership is the main factor that predicts the representational structure of sounds in VOTC in both blind and sighted people, rather than other alternatives related to lower-level attributes of sounds that are at the basis of category selectivity in the temporal cortex (Moerel, De Martino, & Formisano, 2012). These last results elucidate for the first time the computational characteristics that determine the categorical response for sounds in VOTC in sighted and blind people. Finally, our study discloses an interesting dissociation between VOTC and EVC by showing that categorical membership are encoded in the EVC of blind people only, using a representational format that does not relate neither to the acoustic or categorical structure of our stimuli and using a representational format different from the one implemented in VOTC.

Different visual categories elicit distinct distributed responses in VOTC using a remarkable topographic consistency across individuals (Julian et al., 2012; Kanwisher, 2010). It was suggested that regular visual properties specific to each category like retinotopic eccentricity biases (Gomez et al., 2019; Malach et al., 2002), curvature (Nasr et al., 2014) or spatial frequencies (Rajimehr et al., 2011) could drive the development of categorical response in VOTC for visual information (Andrews, Clarke, Pell, & Hartley, 2010; Baldassi et al., 2013; Bracci, Kalfas, & Op de Beeck, 2018; Rice et al., 2014). For instance, the parahippocampal place area (PPA) and the fusiform face area (FFA) receive dominant inputs from downstream regions of the visual system with differential selectivity for high vs low spatial frequencies and peripheral vs. foveal inputs, causing them to respond differentially to place and face stimuli (Levy, Hasson, Avidan, Hendler, & Malach, 2001). These biases for specific visual attributes could be present at birth and represent a proto-organization driving the development of the categorical responses of VOTC based on experience (Arcaro & Livingstone, 2017; Gomez et al., 2019). For instance, a proto-eccentricity map is evident early in infant development (Arcaro & Livingstone, 2017) and monkeys trained early in life to discriminate different categories varying in their curvilinearity/rectilinearity develop distinct and consistent functional clusters for these categories (Srihasam, Vincent, & Livingstone, 2014). Further, adults who had intensive visual experience with Pokémon early in life demonstrate distinct

distributed cortical responses to this trained visual category with a systematic location supposed to be based on retinal eccentricity (Gomez et al., 2019).

Although our results by no means disprove the observations that inherent visual biases can influence the development of the functional topography of high-level vision (Gomez et al., 2019; Hasson, Levy, Behrmann, Hendler, & Malach, 2002; Nasr et al., 2014); our data however suggest that category membership independently of visual attributes is also a key developmental factor that determines the consistent functional topography of the VOTC. Our study demonstrates that VOTC responds to sounds using a similar distributed functional profile to the one found in response to vision, even in case of people that have never had visual experience.

By orthogonalizing category membership and visual features of visual stimuli, previous studies reported a residual categorical effect in VOTC, highlighting how some of the variance in the neural data of VOTC might be explained by high-level categorical properties of the stimuli even when the contribution of the basic low-level features has been controlled for (Bracci & Beeck, 2016; Kaiser, Azzalini, & Peelen, 2016; Proklova, Kaiser, & Peelen, 2016). Category-selectivity has also been observed in VOTC during semantic tasks when word stimuli were used, suggesting an involvement of the occipito-temporal cortex in the retrieval of category-specific conceptual information. Moreover, previous research has shown that learning to associate semantic features (e.g., "floats") and spatial contextual associations (e.g., "found in gardens") with novel objects influence VOTC representations, such that objects with contextual connections exhibited higher pattern similarity after learning in association with a reduction in pattern information about the object's visual features (Clarke, Pell, Ranganath, & Tyler, 2016).

Even if we cannot fully exclude that the processing of auditory information in the VOTC of sighted people could be the by-product of the visual imagery triggered by the non-visual stimulation (Cichy, Heinzle, & Haynes, 2012; Kosslyn, Thompson, Klm, & Alpert, 1995; Reddy, Tsuchiya, & Serre, 2010; Slotnick, Thompson, & Kosslyn, 2005; Stokes, Thompson, Cusack, & Duncan, 2009), we find it unlikely. First, we purposely included two separate groups of sighted people, each one performing the experiment in one modality only, in order to minimize the

influence of having heard or seen the stimuli in the other modality in the context of the experiment. Also, we used a fast presentation of the stimuli, that restricted the time window to build a visual image of the actual sound since the next sound was presented quickly after (Logie, 1989). Finally, we would expect that visual imagery would also triggers information to be processed in posterior occipital regions (Kosslyn et al., 1999). Instead, we found that EVC does not discriminate the different sounds in the sighted group (fig. 2B and fig. 3A), making the visual imagery hypothesis unlikely to explain our results.

Comparing blind and sighted individuals arguably provides the strongest evidence for the hypothesis that category-selective regions traditionally considered to be "high-level visual regions" can develop independently of visual experience. Interestingly, we found that the decoding accuracy for the auditory categories in VOTC is significantly higher in the early blind compared to the sighted control group (Fig. 2B). In addition, the correlation between the topographic distribution of categorical response observed in VOTC was stronger in blind versus sighted people (Fig. 1B). Moreover, the correlation between the representational structure of visual and auditory categories is almost double in the blind when compared to the sighted group (Fig. 3-panel A2). Finally, the representation for the auditory stimuli in VOTC is more similar between blind than between sighted subjects (fig. 5), showing an increased inter-subject stability of the representation in case of early visual deprivation. All together, these results not only demonstrate that a categorical organization similar to the one found in vision could emerge in VOTC in absence of visual experience, but also that such categorical response to sounds is actually enhanced and more stable in congenitally blind people.

Several studies have shown that in absence of vision, the occipital cortex enhances its response to non-visual information processing (Collignon et al., 2012, 2011; Pietrini et al., 2004; Sadato et al., 1998; Weeks et al., 2000). However, people debate on the mechanistic principles guiding the expression of this crossmodal plasticity. For instance, it was suggested that early visual deprivation changes the computational nature of the occipital cortex which would reorganize itself for higher-level functions, distant from the ones typically implemented for visual stimuli in the

same region (Bedny, 2017). In contrast with this view, our results demonstrate that the expression of crossmodal plasticity, at least in VOTC (see differences in EVC below), is constrained by the inherent categorical structure endowed in this region. First, we highlighted remarkably similar functional profile of VOTC for visual and auditory stimuli in sighted and in early blind individuals (Fig. 3B). In addition, we showed that VOTC is encoding a similar categorical dimension of the stimuli across different inputs of presentation and different visual experiences (Fig. 4B). In support of such idea, we recently demonstrated that the involvement of right dorsal occipital region for arithmetic processing in blind people actually relates to the intrinsic "spatial" nature of these regions, a process involved in specific arithmetic computation (e.g. subtraction but not multiplication) (Crollen et al., 2019). Similarly, the involvement of VOTC during "language" as observed in previous studies (Bedny, Pascual-Leone, Dodell-Feder, Fedorenko, & Saxe, 2011; Burton, McLaren, & Sinclair, 2006; Kim, Kanjlia, Merabet, & Bedny, 2017; Lane, Kanjlia, Omaki, & Bedny, 2015; Röder, Stock, Bien, Neville, & Rösler, 2002) may relate to the fact that some level of representation involved in language (e.g. semantic) can be intrinsically encoded in VOTC as supported by the current results (Huth, De Heer, Griffiths, Theunissen, & Gallant, 2016). In fact, we suggest that VOTC regions have innate predispositions relevant to important categorical distinctions that cause category-selective patches to emerge regardless of sensory experience. Why would the "visual" system embed representation of categories independently of their perceptual features? One argument might be that items from a particular broad category (e.g. inanimate) are so diverse that they may not share systematic perceptual features and therefore a higher-level of representation, partially abstracted from vision, might prove important. Indeed, we gather evidence in support of an extension of the intrinsic categorical organization of VOTC that is already partially independent from vision in sighted. This finding represents an important step forward in understanding how experience and intrinsic constraints interact in shaping the functional properties of VOTC. An intriguing possibility raised by our results is that the crossmodal plasticity observed in early blind individuals may actually serve to maintain the functional homeostasis of occipital regions.

What would be the mechanism driving the preservation of the categorical organization of VOTC in case of congenital blindness? It is thought that the specific topographic location of a selective brain functions is constrained by an innate profile of functional and structural connections with extrinsic brain regions (Passingham et al., 2002). Since the main fiber tracts are already present in full-term human neonates (Dubois et al., 2014; Jessica Dubois, Adibpour, Poupon, Hertz-Pannier, & Dehaene-Lambertz, 2016; Kennedy et al., 1999; Kostović & Judaš, 2010; Marín-Padilla, 2011; Takahashi, Sakurai, Davis, & Buxbaum, 2011), such initial connectome may at least partly drive the functional development of a specific area. Supporting this hypothesis, the visual word form area (VWFA) in VOTC shows robust and specific anatomical connectivity to EVC and to frontotemporal language networks and this connectivity fingerprint can predict the location of VWFA even before a child learn to read (Saygin et al., 2016). Similarly, anatomical connectivity profile can predict the location of the fusiform face area (FFA) (Saygin et al., 2012). In addition to intra-occipital connections, FFA has a direct structural connection with the temporal voice area (TVA) in the superior temporal sulcus (Benetti et al., 2018; Blank, Anwander, & von Kriegstein, 2011) thought to support similar computations applied on faces and voices as well as their integration (Von Kriegstein, Kleinschmidt, Sterzer, & Giraud, 2005). Interestingly, recent studies suggested that the maintenance of those selective structural connections between TVA and FFA explain the preferential recruitment of TVA for face processing in congenitally deaf people (Benetti et al., 2018, 2017). This TVA-FFA connectivity may explain why voices preferentially map slightly more lateral to the mid-fusiform sulcus (Fig. 1B) (Hurk et al., 2017). Similarly, sounds of big objects or natural scenes preferentially recruit more mesial VOTC regions (Fig. 1B), overlapping with the parahippocampal place area, potentially due to the preserved pattern of structural connectivity of those regions in blind people (Wang et al., 2017). The existence of these innate large-scale brain connections that are specific for each region supporting separate categorical domain may provide the structural scaffolding on which crossmodal inputs capitalizes to reach VOTC in both sighted and blind people, potentially through feed-back connections. Indeed, it has been shown that the main white

matter tracks including those involving occipital regions are not significantly different between blind and sighted individuals (Shimony et al., 2006). In EB, the absence of competitive visual inputs typically coming from feed-forward inputs from EVC may actually trigger an enhanced weighting of those feed-back inter-modal connection leading to an extension of selective categorical response to sounds in VOTC, as observed in the current study. Our results provide crucial support for this "biased connectivity" hypothesis (Hannagan, Amedi, Cohen, Dehaene-lambertz, & Dehaene, 2015; Mahon & Caramazza, 2011) showing that VOTC subregions are part of a large-scale functional network representing categorical information in a format that is at least partially independent from the modality of the stimuli presentation and from the visual experience.

A different profile emerged from the more posterior portion of the occipital cortex. First, sound categories could be decoded in the EVC of EB (Fig. 2B) but not in the SC. In addition, the representational structure of EVC for sounds correlated to the one found in vision only in EB (Fig. 3 – Panel A2). However, neither the categorical membership nor the acoustic attributes of sounds correlated with the representational structure found in the EVC of EB (Fig. 3B). A possible explanation for this result is that the posterior part of the occipital cortex in EB is the region that distance itself the most from the native computation it typically implements (Bi, Wang, & Caramazza, 2016; Büchel, 2003; Wang et al., 2015). Because this area has a native computation that does not easily transfer to another sensory modality, it may therefore rewire itself for distant functions (Bedny, 2017). Some studies, for instance reported an involvement of EVC in high-level linguistic tasks (Ackeren et al., 2018; Amedi, Raz, Pianka, Malach, & Zohary, 2003; Bedny et al., 2011). However, as demonstrated here, the categorical membership of sounds, which may be a proxy for semantic representation, does not explain the representational structure of EVC in our study. It would be interesting to investigate whether models based on linguistic properties such as word frequency or distributional statistic in language corpus (Baroni, Bernardini, Ferraresi, & Zanchetta, 2009) would, at least partially, explain the enhanced information that we found in EVC of EB. However, our design does not allow us to implement this analysis because the language-statistic DSM

based on our stimuli space highly correlate with categorical models. Future studies should investigate this point using a set of stimuli in which the categorical and the linguistic dimensions should be orthogonalized.

References

Ackeren, M. J. Van, Barbero, F. M., Mattioni, S., Bottini, R., Van Ackeren, M. J., Barbero, F. M., Collignon, O. (2018). Neuronal populations in the occipital cortex of the blind synchronize to the temporal dynamics of speech. *ELife*, *7*, 1–20. https://doi.org/10.7554/eLife.31640

Amedi, A., Raz, N., Azulay, H., Malach, R., & Zohary, E. (2010). Cortical activity during tactile exploration of objects in blind and sighted humans. *Restorative Neurology and Neuroscience*, *28*(2), 143–156. https://doi.org/10.3233/RNN-2010-0503

Amedi, A., Raz, N., Pianka, P., Malach, R., & Zohary, E. (2003). Early "visual" cortex activation correlates with superior verbal memory performance in the blind. *Nature Neuroscience*, *6*(7), 758–766. https://doi.org/10.1038/nn1072

Amedi, A., Stern, W. M., Camprodon, J. a, Bermpohl, F., Merabet, L., Rotman, S., Pascual-Leone, A. (2007). Shape conveyed by visual-to-auditory sensory substitution activates the lateral occipital complex. *Nature Neuroscience*, *10*(6), 687–689. https://doi.org/10.1038/nn1912

Andrews, T. J., Clarke, A., Pell, P., & Hartley, T. (2010). Selectivity for low-level features of objects in the human ventral stream. *NeuroImage*, *49*(1), 703–711. https://doi.org/10.1016/j.neuroimage.2009.08.046

Arcaro, M. J., & Livingstone, M. S. (2017). A hierarchical, retinotopic proto-organization of the primate visual system at birth. *ELife*, *6*. https://doi.org/10.7554/eLife.26196

Ashburner, J. (2007). A fast diffeomorphic image registration algorithm. *NeuroImage*, *38*(1), 95–113. https://doi.org/10.1016/j.neuroimage.2007.07.007

Baldassi, C., Alemi-Neissi, A., Pagan, M., DiCarlo, J. J., Zecchina, R., & Zoccolan, D. (2013). Shape Similarity, Better than Semantic Membership, Accounts for the

Structure of Visual Object Representations in a Population of Monkey Inferotemporal Neurons. *PLoS Computational Biology*, *9*(8). https://doi.org/10.1371/journal.pcbi.1003167

Baroni, M., Bernardini, S., Ferraresi, A., & Zanchetta, E. (2009). The waCky wide web: A collection of very large linguistically processed web-crawled corpora. *Language Resources and Evaluation*, *43*(3), 209–226. https://doi.org/10.1007/s10579-009-9081-4

Bavelier, D., & Neville, H. J. (2002). Cross-modal plasticity: where and how? *Nature Reviews. Neuroscience*, *3*(6), 443–452. https://doi.org/10.1038/nrn848

Bedny, M. (2017). Evidence from Blindness for a Cognitively Pluripotent Cortex. *Trends in Cognitive Sciences*, *21*(9), 637–648. https://doi.org/10.1016/j.tics.2017.06.003

Bedny, M., Pascual-Leone, A., Dodell-Feder, D., Fedorenko, E., & Saxe, R. (2011). Language processing in the occipital cortex of congenitally blind adults. *Proceedings of the National Academy of Sciences of the United States of America*, *108*(11), 4429–4434. https://doi.org/10.1073/pnas.1014818108

Behrens, T. E. J., & Sporns, O. (2012). Human connectomics. *Current Opinion in Neurobiology*. https://doi.org/10.1016/j.conb.2011.08.005

Benetti, S., Novello, L., Maffei, C., Rabini, G., Jovicich, J., & Collignon, O. (2018). White matter connectivity between occipital and temporal regions involved in face and voice processing in hearing and early deaf individuals. *NeuroImage*, *179*(June), 263–274. https://doi.org/10.1016/j.neuroimage.2018.06.044

Benetti, S., van Ackeren, M. J., Rabini, G., Zonca, J., Foa, V., Baruffaldi, F., Collignon, O. (2017). Functional selectivity for face processing in the temporal voice area of early deaf individuals. *Proceedings of the National Academy of Sciences*, *114*(31), E6437–E6446. https://doi.org/10.1073/pnas.1618287114

Bi, Y., Wang, X., & Caramazza, A. (2016). Object Domain and Modality in the Ventral Visual Pathway. *Trends in Cognitive Sciences*, *20*(4), 282–290. https://doi.org/10.1016/j.tics.2016.02.002

Blank, H., Anwander, A., & von Kriegstein, K. (2011). Direct Structural Connections between Voice- and Face-Recognition Areas. *Journal of Neuroscience*, *31*(36),

12906–12915. https://doi.org/10.1523/JNEUROSCI.2091-11.2011

Borghesani, V., Pedregosa, F., Buiatti, M., Amadon, A., Eger, E., & Piazza, M. (2016). Word meaning in the ventral visual path: a perceptual to conceptual gradient of semantic coding. *NeuroImage*. https://doi.org/10.1016/j.neuroimage.2016.08.068

Bracci, S., & Op de Beeck, H. (2016). Dissociations and Associations between Shape and Category Representations in the Two Visual Pathways, *36*(2), 432–444. https://doi.org/10.1523/JNEUROSCI.2314-15.2016

Bracci, S., Kalfas, I., & Op de Beeck, H. (2018). The ventral visual pathway represents animal appearance rather than animacy, unlike human behavior and deep neural networks. *Journal of Vision*, *18*(10), 552. https://doi.org/10.1167/18.10.552

Büchel, C. (2003). Cortical hierarchy turned on its head. *Nature Neuroscience*, *6*(7), 657–658. https://doi.org/10.1038/nn0703-657

Burton, H., McLaren, D. G., & Sinclair, R. J. (2006). Reading embossed capital letters: an fMRI study in blind and sighted individuals. *Human Brain Mapping*, *27*(4), 325–339. https://doi.org/10.1002/hbm.20188

Carlson, T., Tovar, D. A., Alink, A., & Kriegeskorte, N. (2013). Representational dynamics of object vision: the first 1000 ms. *Journal of Vision*. https://doi.org/10.1167/13.10.1

Cichy, Radoslaw M., Heinzle, J., & Haynes, J. D. (2012). Imagery and perception share cortical representations of content and location. *Cerebral Cortex*, *22*(2), 372–380. https://doi.org/10.1093/cercor/bhr106

Cichy, Radoslaw M., & Pantazis, D. (2017). Multivariate pattern analysis of MEG and EEG: A comparison of representational structure in time and space. *NeuroImage*. https://doi.org/10.1016/j.neuroimage.2017.07.023

Cichy, Radoslaw M., Sterzer, P., Heinzle, J., Elliott, L. T., Ramirez, F., & Haynes, J. D. (2013). Probing principles of large-scale object representation: Category preference and location encoding. *Human Brain Mapping*, *34*(7), 1636–1651. https://doi.org/10.1002/hbm.22020

Clarke, A., Pell, P. J., Ranganath, C., & Tyler, L. K. (2016). Learning warps object

representations in the ventral temporal cortex. *Journal of Cognitive Neuroscience*. https://doi.org/10.1162/jocn_a_00951

Collignon, O., Dormal, G., & Lepore, F. (2012). Building the Brain in the Dark: Functional and Specific Crossmodal Reorganization in the Occipital Cortex of Blind Individuals. *Plasticity in Sensory Systems*, 73–96.

Collignon, O., Vandewalle, G., Voss, P., Albouy, G., Charbonneau, G., Lassonde, M., & Lepore, F. (2011). Functional specialization for auditory-spatial processing in the occipital cortex of congenitally blind humans. *Proceedings of the National Academy of Sciences of the United States of America*, *108*(11), 4435–4440. https://doi.org/10.1073/pnas.1013928108

Crollen, V., Lazzouni, L., Rezk, M., Bellemare, A., Lepore, F., Noël, M. P., Collignon, O. (2019). Recruitment of the occipital cortex by arithmetic processing follows computational bias in the congenitally blind. *NeuroImage*. https://doi.org/10.1016/j.neuroimage.2018.11.034

Desikan, R. S., Ségonne, F., Fischl, B., Quinn, B. T., Dickerson, B. C., Blacker, D., Killiany, R. J. (2006). An automated labeling system for subdividing the human cerebral cortex on MRI scans into gyral based regions of interest. *NeuroImage*, *31*(3), 968–980. https://doi.org/10.1016/j.neuroimage.2006.01.021

Dobs, K., Isik, L., Pantazis, D., & Kanwisher, N. (2019). How face perception unfolds over time. *Nature Communications*. https://doi.org/10.1038/s41467-019-09239-1

Dormal, G., & Collignon, O. (2011). Functional selectivity in sensory-deprived cortices. *Journal of Neurophysiology*, *105*(6), 2627–2630. https://doi.org/10.1152/jn.00109.2011

Dormal, G., Rezk, M., Yakobov, E., Lepore, F., & Collignon, O. (2016). NeuroImage Auditory motion in the sighted and blind : Early visual deprivation triggers a large-scale imbalance between auditory and " visual " brain regions. *NeuroImage*, *134*, 630–644. https://doi.org/10.1016/j.neuroimage.2016.04.027

Downing, P. E., Downing, P. E., Jiang, Y., Jiang, Y., Shuman, M., Shuman, M., … Kanwisher, N. (2001). A cortical area selective for visual processing of the human body. *Science (New York, N.Y.)*, *293*(5539), 2470–2473.

https://doi.org/10.1126/science.1063414

Dubois, J., Dehaene-Lambertz, G., Kulikova, S., Poupon, C., Hüppi, P. S., & Hertz-Pannier, L. (2014). The early development of brain white matter: A review of imaging studies in fetuses, newborns and infants. *Neuroscience*. https://doi.org/10.1016/j.neuroscience.2013.12.044

Dubois, Jessica, Adibpour, P., Poupon, C., Hertz-Pannier, L., & Dehaene-Lambertz, G. (2016). MRI and M/EEG studies of the White Matter Development in Human Fetuses and Infants: Review and Opinion. *Brain Plasticity*, *2*(1), 49–69. https://doi.org/10.3233/bpl-160031

Epstein, R., & Kanwisher, N. (1998). A cortical representation of the local visual environment. *Nature*, *392*(6676), 598–601. https://doi.org/10.1038/33402

Etzel, J. A., Zacks, J. M., & Braver, T. S. (2013). Searchlight analysis: Promise, pitfalls, and potential. *NeuroImage*. https://doi.org/10.1016/j.neuroimage.2013.03.041

Giordano, B. L., McAdams, S., Zatorre, R. J., Kriegeskorte, N., & Belin, P. (2013). Abstract encoding of auditory objects in cortical activity patterns. *Cerebral Cortex (New York, N.Y. : 1991)*, *23*(9), 2025–2037. https://doi.org/10.1093/cercor/bhs162

Gomez, J., Barnett, M., & Grill-Spector, K. (2019). Extensive childhood experience with Pokémon suggests eccentricity drives organization of visual cortex. *Nature Human Behaviour*. https://doi.org/10.1038/s41562-019-0592-8

Handjaras, G., Ricciardi, E., Leo, A., Lenci, A., Cecchetti, L., Cosottini, M., Pietrini, P. (2016). How concepts are encoded in the human brain: A modality independent, category-based cortical organization of semantic knowledge. *NeuroImage*, *135*, 232–242. https://doi.org/http://dx.doi.org/10.1016/j.neuroimage.2016.04.063

Hannagan, T., Amedi, A., Cohen, L., Dehaene-lambertz, G., & Dehaene, S. (2015). Origins of the specialization for letters and numbers in ventral occipitotemporal cortex. *Trends in Cognitive Sciences*, 1–9. https://doi.org/10.1016/j.tics.2015.05.006

Hasson, U., Levy, I., Behrmann, M., Hendler, T., & Malach, R. (2002). Eccentricity bias as an organizing principle for human high-order object areas. *Neuron*,

34(3), 479–490. Retrieved from http://www.ncbi.nlm.nih.gov/pubmed/11988177

Haxby, Gobbini, Furey, Ishai, Schouten, & Pietrini. (2001). Distributed and overlapping representations of faces and objects in ventral temporal cortex. *Science (New York, N.Y.)*, *293*(5539), 2425–2430. https://doi.org/10.1126/science.1063736

Haxby, J. V., Connolly, A. C., & Guntupalli, J. S. (2014). Decoding Neural Representational Spaces Using Multivariate Pattern Analysis. *Annual Review of Neuroscience*, *37*(1), 435–456. https://doi.org/10.1146/annurev-neuro-062012-170325

Haxby, J. V, Guntupalli, J. S., Connolly, A. C., Halchenko, Y. O., Conroy, B. R., Gobbini, M. I.,Ramadge, P. J. (2011). A Common , High-Dimensional Model of the Representational Space in Human Ventral Temporal Cortex. *Neuron, 72(2),* 404-416. https://doi.org/10.1016/j.neuron.2011.08.026

He, C., Peelen, M. V, Han, Z., Lin, N., Caramazza, A., & Bi, Y. (2013). Selectivity for large nonmanipulable objects in scene-selective visual cortex does not require visual experience. *NeuroImage*, *79*, 1– https://doi.org/10.1016/j.neuroimage.2013.04.051

Hubel, D. H., & Wiesel, T. N. (1962). Receptive fields, binocular interaction and functional architecture in the cat's visual cortex. *The Journal of Physiology*. https://doi.org/10.1113/jphysiol.1962.sp006837

Huber, E., Jiang, F., & Fine, I. (2019). Responses in area hMT+ reflect tuning for both auditory frequency and motion after blindness early in life. *Proceedings of the National Academy of Sciences*, (7), 201815376. https://doi.org/10.1073/pnas.1815376116

van den Hurk, J., Van Baelen, M., & de Beeck, H.P.O. (2017). Development of visual category selectivity in ventral visual cortex does not require visual experience, 1–10. https://doi.org/10.1073/pnas.1612862114

Huth, A. G., De Heer, W. A., Griffiths, T. L., Theunissen, F. E., & Gallant, J. L. (2016). Natural speech reveals the semantic maps that tile human cerebral cortex. *Nature*. https://doi.org/10.1038/nature17637

Jiang, J., Zhu, W., Shi, F., Liu, Y., Li, J., Qin, W., Jiang, T. (2009). Thick Visual Cortex in the Early Blind. *Journal of Neuroscience*, *29*(7), 2205–2211. https://doi.org/10.1523/JNEUROSCI.5451-08.2009

Julian, J. B., Fedorenko, E., Webster, J., & Kanwisher, N. (2012). An algorithmic method for functionally defining regions of interest in the ventral visual pathway. *NeuroImage*, *60*(4), 2357–2364. https://doi.org/10.1016/j.neuroimage.2012.02.055

Kaiser, D., Azzalini, D. C., & Peelen, M. V. (2016). Shape-independent object category responses revealed by MEG and fMRI decoding. *Journal of Neurophysiology*. https://doi.org/10.1152/jn.01074.2015

Kanwisher, N. (2010). Functional specificity in the human brain: A window into the functional architecture of the mind. *Proceedings of the National Academy of Sciences*, *107*(25), 11163–11170. https://doi.org/10.1073/pnas.1005062107

Kanwisher, N., McDermott, J., & Chun, M. M. (1997). The fusiform face area: a module in human extrastriate cortex specialized for face perception. *The Journal of Neuroscience : The Official Journal of the Society for Neuroscience*.

Kennedy, D. N., O'Craven, K. M., Ticho, B. S., Goldstein, A. M., Makris, N., & Henson, J. W. (1999). Structural and functional brain asymmetries in human situs inversus totalis. *Neurology*.

Khaligh-Razavi, S. M., & Kriegeskorte, N. (2014). Deep Supervised, but Not Unsupervised, Models May Explain IT Cortical Representation. *PLoS Computational Biology*, *10*(11). https://doi.org/10.1371/journal.pcbi.1003915

Kim, J. S., Kanjlia, S., Merabet, L. B., & Bedny, M. (2017). Development of the Visual Word Form Area Requires Visual Experience: Evidence from Blind Braille Readers. *The Journal of Neuroscience*, *37*(47), 11495–11504. https://doi.org/10.1523/jneurosci.0997-17.2017

Kitada, X. R., Yoshihara, K., Sasaki, A. T., Hashiguchi, M., Kochiyama, T., & Sadato, X. N. (2014). The Brain Network Underlying the Recognition of Hand Gestures in the Blind : The Supramodal Role of the Extrastriate Body Area, *34*(30), 10096–10108. https://doi.org/10.1523/JNEUROSCI.0500-14.2014

Kosslyn, S. M., Pascual-Leone, A., Felician, O., Camposano, S., Keenan, J. P.,

Thompson, W. L., … Alpert, N. M. (1999). The role of area 17 in visual imagery: Convergent evidence from PET and rTMS. *Science*. https://doi.org/10.1126/science.284.5411.167

Kosslyn, Stephen M., Thompson, W. L., Klm, I. J., & Alpert, N. M. (1995). Topographical representations of mental images in primary visual cortex. *Nature*, *378*(6556), 496–498. https://doi.org/10.1038/378496a0

Kostović, I., & Judaš, M. (2010). The development of the subplate and thalamocortical connections in the human foetal brain. *Acta Paediatrica, International Journal of Paediatrics*. https://doi.org/10.1111/j.1651-2227.2010.01811.x

Kriegeskorte, N., Mur, M., & Bandettini, P. (2008). Representational similarity analysis - connecting the branches of systems neuroscience. *Frontiers in Systems Neuroscience*, *2*(November), 4. https://doi.org/10.3389/neuro.06.004.2008

Kriegeskorte, N., Mur, M., Ruff, D. A., Kiani, R., Bodurka, J., Esteky, H., … Bandettini, P. A. (2008). Matching Categorical Object Representations in Inferior Temporal Cortex of Man and Monkey. *Neuron*, *60*(6), 1126–1141. https://doi.org/10.1016/j.neuron.2008.10.043

Lane, C., Kanjlia, S., Omaki, A., & Bedny, M. (2015). "Visual" Cortex of Congenitally Blind Adults Responds to Syntactic Movement. *Journal of Neuroscience*, *35*(37), 12859–12868. https://doi.org/10.1523/JNEUROSCI.1256-15.2015

Leaver, A. M., & Rauschecker, J. P. (2010). Cortical representation of natural complex sounds: effects of acoustic features and auditory object category. *The Journal of Neuroscience : The Official Journal of the Society for Neuroscience*, *30*(22), 7604–7612. https://doi.org/10.1523/JNEUROSCI.0296-10.2010

Levy, I., Hasson, U., Avidan, G., Hendler, T., & Malach, R. (2001). Center-periphery organization of human object areas. *Nature Neuroscience*. https://doi.org/10.1038/87490

Logie, R. H. (1989). Characteristics of visual short-term memory. *European Journal of Cognitive Psychology*, *1*(4), 275–284. https://doi.org/10.1080/09541448908403088

Mahon, B. Z., & Caramazza, A. (2011). What drives the organization of object knowledge in the brain? *Trends in Cognitive Sciences*, *15*(3), 97–103. https://doi.org/10.1016/j.tics.2011.01.004

Malach, R., Levy, I., & Hasson, U. (2002). The topography of high-order human object areas. *Trends in Cognitive Sciences*.

Marín-Padilla, M. (2011). The human brain: Prenatal development and structure. *The Human Brain: Prenatal Development and Structure*, 1–145. https://doi.org/10.1007/978-3-642-14724-1

Martin, C., Douglas, D., Newsome, R., Man, L., & Barense, M. (2017). Integrative and distintive coding of perceptual and concptual features in the ventral stream. *ELife*, 1–29. https://doi.org/10.7554/eLife.31873

McCandliss, B. D., Cohen, L., & Dehaene, S. (2003). The visual word form area: Expertise for reading in the fusiform gyrus. *Trends in Cognitive Sciences*. https://doi.org/10.1016/S1364-6613(03)00134-7

Moerel, M., De Martino, F., & Formisano, E. (2012). Processing of Natural Sounds in Human Auditory Cortex: Tonotopy, Spectral Tuning, and Relation to Voice Sensitivity. *Journal of Neuroscience*. https://doi.org/10.1523/jneurosci.1388-12.2012

Moerel, M., De Martino, F., & Formisano, E. (2012). Behavioral/Systems/Cognitive Processing of Natural Sounds in Human Auditory Cortex: Tonotopy, Spectral Tuning, and Relation to Voice Sensitivity. *The Journal of Neuroscience*, *32*(41), 14205–14216. https://doi.org/10.1523/JNEUROSCI.1388-12.2012

Nasr, S., Echavarria, C. E., & Tootell, R. B. H. (2014). Thinking Outside the Box: Rectilinear Shapes Selectively Activate Scene-Selective Cortex. *Journal of Neuroscience*. https://doi.org/10.1523/jneurosci.4802-13.2014

Neville, H., & Bavelier, D. (2002). Human brain plasticity: evidence from sensory deprivation and altered language experience. *Progress in Brain Research*, *138*, 177–188. https://doi.org/10.1016/S0079-6123(02)38078-6

Nili, H., Wingfield, C., Walther, A., Su, L., Marslen-Wilson, W., & Kriegeskorte, N. (2014). A toolbox for representational similarity analysis. *PLoS Computational Biology*, *10*(4), e1003553. https://doi.org/10.1371/journal.pcbi.1003553

Norman, K. a, Polyn, S. M., Detre, G. J., & Haxby, J. V. (2006). Beyond mind-reading: multi-voxel pattern analysis of fMRI data. *Trends in Cognitive Sciences*, *10*(9), 424–430. https://doi.org/10.1016/j.tics.2006.07.005

O'Toole, A. J., Jiang, F., Abdi, H., & Haxby, J. V. (2005). Partially distributed representations of objects and faces in ventral temporal cortex. *Journal of Cognitive Neuroscience*, *17*(4), 580–590. https://doi.org/10.1162/0898929053467550

Pan, W. J., Wu, G., Li, C. X., Lin, F., Sun, J., & Lei, H. (2007). Progressive atrophy in the optic pathway and visual cortex of early blind Chinese adults: A voxel-based morphometry magnetic resonance imaging study. *NeuroImage*, *37*(1), 212–220. https://doi.org/10.1016/j.neuroimage.2007.05.014

Park, H., Doo, J., Yeop, E., Park, B., Oh, M., Lee, S., & Kim, J. (2009). NeuroImage Morphological alterations in the congenital blind based on the analysis of cortical thickness and surface area ☆. *NeuroImage*, *47*(1), 98–106. https://doi.org/10.1016/j.neuroimage.2009.03.076

Passingham, R. E., Stephan, K. E., & Kötter, R. (2002). The anatomical basis of functional localization in the cortex. *Nature Reviews Neuroscience*. https://doi.org/10.1038/nrn893

Peelen, M., Bracci, S., Lu, X., He, C., Caramazza, A., & Bi, Y. (2013). Tool selectivity in left occipitotemporal cortex develops without vision, 1–10. https://doi.org/10.1162/jocn

Peelen, M. V., & Downing, P. E. (2017). Category selectivity in human visual cortex: Beyond visual object recognition. *Neuropsychologia*, *105*(April), 177–183. https://doi.org/10.1016/j.neuropsychologia.2017.03.033

Peelen, M. V., He, C., Han, Z., Caramazza, A., & Bi, Y. (2014). Nonvisual and visual object shape representations in occipitotemporal cortex: evidence from congenitally blind and sighted adults. *The Journal of Neuroscience : The Official Journal of the Society for Neuroscience*, *34*(1), 163–170. https://doi.org/10.1523/JNEUROSCI.1114-13.2014

Pereira, F., Mitchell, T., & Botvinick, M. (2009). Machine learning classifiers and fMRI: a tutorial overview. *NeuroImage*.

https://doi.org/10.1016/j.neuroimage.2008.11.007

Pietrini, P., Furey, M. L., Ricciardi, E., Gobbini, M. I., Wu, W.-H. C., Cohen, L., … Haxby, J. V. (2004). Beyond sensory images: Object-based representation in the human ventral pathway. *Proceedings of the National Academy of Sciences of the United States of America*, *101*(15), 5658–5663. https://doi.org/10.1073/pnas.0400707101

Pillet, I., Beeck, H. Op De, & Masson, H. L. (2018). Comparing the functional structure of neural networks from representational similarity analysis with those from functional connectivity and univariate analyses * Correspondence : *Biorxiv*. https://doi.org/https://doi.org/10.1101/487199

Poirier, C., Collignon, O., Scheiber, C., & Volder, a. (2004). Auditory motion processing in early blind subjects. *Cognitive Processing*, *5*(4), 254–256. https://doi.org/10.1007/s10339-004-0031-1

Proklova, D., Kaiser, D., & Peelen, M. V. (2016). Disentangling representations of object shape and object category in human visual cortex: The animate-inanimate distinction. *Journal of Cognitive Neuroscience*. https://doi.org/10.1162/jocn_a_00924

Proklova, D., Kaiser, D., & Peelen, M. V. (2019). MEG sensor patterns reflect perceptual but not categorical similarity of animate and inanimate objects. *NeuroImage*, (725970), 1–21. https://doi.org/10.1101/238584

Rajimehr, R., Devaney, K. J., Bilenko, N. Y., Young, J. C., & Tootell, R. B. H. (2011). The "parahippocampal place area" responds preferentially to high spatial frequencies in humans and monkeys. *PLoS Biology*, *9*(4), e1000608. https://doi.org/10.1371/journal.pbio.1000608

Reddy, L., Tsuchiya, N., & Serre, T. (2010). Reading the mind's eye: Decoding category information during mental imagery. *NeuroImage*, *50*(2), 818–825. https://doi.org/10.1016/j.neuroimage.2009.11.084

Reich, L., Szwed, M., Cohen, L., & Amedi, A. (2011). A ventral visual stream reading center independent of visual experience. *Current Biology : CB*, *21*(5), 363–368. https://doi.org/10.1016/j.cub.2011.01.040

Ricciardi, E., Vanello, N., Sani, L., Gentili, C., Scilingo, E. P., Landini, L., … Pietrini, P.

(2007). The effect of visual experience on the development of functional architecture in hMT+. *Cerebral Cortex (New York, N.Y. : 1991)*, *17*(12), 2933–2939. https://doi.org/10.1093/cercor/bhm018

Rice, G. E., Watson, D. M., Hartley, T., & Andrews, T. J. (2014). Low-Level Image Properties of Visual Objects Predict Patterns of Neural Response across Category-Selective Regions of the Ventral Visual Pathway. *The Journal of Neuroscience : The Official Journal of the Society for Neuroscience*, *34*(26), 8837–8844. https://doi.org/10.1523/JNEUROSCI.5265-13.2014

Röder, B., Stock, O., Bien, S., Neville, H., & Rösler, F. (2002). Speech processing activates visual cortex in congenitally blind humans. *European Journal of Neuroscience*, *16*(5), 930–936. https://doi.org/10.1046/j.1460-9568.2002.02147.x

Sadato, N., Pascual-Leone, A., Grafman, J., Deiber, M. P., Ibañez, V., & Hallett, M. (1998). Neural networks for Braille reading by the blind. *Brain*, *121*(7), 1213–1229. https://doi.org/10.1093/brain/121.7.1213

Saygin, Z. M., Osher, D. E., Koldewyn, K., Reynolds, G., Gabrieli, J. D. E., & Saxe, R. R. (2012). Anatomical connectivity patterns predict face selectivity in the fusiform gyrus. *Nature Neuroscience*. https://doi.org/10.1038/nn.3001

Saygin, Z. M., Osher, D. E., Norton, E. S., Youssoufian, D. A., Beach, S. D., Feather, J., … Kanwisher, N. (2016). Connectivity precedes function in the development of the visual word form area. *Nature Neuroscience*. https://doi.org/10.1038/nn.4354

Serre, T., Wolf, L., Bileschi, S., Riesenhuber, M., & Poggio, T. (2007). Robust object recognition with cortex-like mechanisms. *IEEE Transactions on Pattern Analysis and Machine Intelligence*. https://doi.org/10.1109/TPAMI.2007.56

Shimony, J. S., Burton, H., Epstein, a a, McLaren, D. G., Sun, S. W., & Snyder, a Z. (2006). Diffusion tensor imaging reveals white matter reorganization in early blind humans. *Cerebral Cortex (New York, N.Y. : 1991)*, *16*(11), 1653–1661. https://doi.org/10.1093/cercor/bhj102

Slotnick, S. D., Thompson, W. L., & Kosslyn, S. M. (2005). Visual mental imagery induces retinotopically organized activation of early visual areas. *Cerebral*

Cortex, *15*(10), 1570–1583. https://doi.org/10.1093/cercor/bhi035

Srihasam, K., Vincent, J. L., & Livingstone, M. S. (2014). Novel domain formation reveals proto-architecture in inferotemporal cortex. *Nature Neuroscience*. https://doi.org/10.1038/nn.3855

Stokes, M., Thompson, R., Cusack, R., & Duncan, J. (2009). Top-Down Activation of Shape-Specific Population Codes in Visual Cortex during Mental Imagery. *Journal of Neuroscience*, *29*(5), 1565–1572. https://doi.org/10.1523/JNEUROSCI.4657-08.2009

Striem-Amit, E., & Amedi, A. (2014). Visual cortex extrastriate body-selective area activation in congenitally blind people "seeing" by using sounds. *Current Biology : CB*, *24*(6), 687–692. https://doi.org/10.1016/j.cub.2014.02.010

Striem-Amit, E., Cohen, L., Dehaene, S., & Amedi, A. (2012). Reading with Sounds: Sensory Substitution Selectively Activates the Visual Word Form Area in the Blind. *Neuron*, *76*(3), 640–652. https://doi.org/10.1016/j.neuron.2012.08.026

Striem-Amit, E., Wang, X., Bi, Y., & Caramazza, A. (2018). Neural representation of visual concepts in people born blind. *Nature Communications*, *9*(1), 1–12. https://doi.org/10.1038/s41467-018-07574-3

Takahashi, N., Sakurai, T., Davis, K. L., & Buxbaum, J. D. (2011). Linking oligodendrocyte and myelin dysfunction to neurocircuitry abnormalities in schizophrenia. *Progress in Neurobiology*. https://doi.org/10.1016/j.pneurobio.2010.09.004

Tong, F., Nakayama, K., Moscovitch, M., Weinrib, O., & Kanwisher, N. (2000). RESPONSE PROPERTIES OF THE HUMAN FUSIFORM FACE AREA. *Cognitive Neuropsychology*, *17*(1–3), 257–280. https://doi.org/10.1080/026432900380607

Von Kriegstein, K., Kleinschmidt, A., Sterzer, P., & Giraud, A. L. (2005). Interaction of face and voice areas during speaker recognition. *Journal of Cognitive Neuroscience*. https://doi.org/10.1162/0898929053279577

Walther, A., Nili, H., Ejaz, N., Alink, A., Kriegeskorte, N., & Diedrichsen, J. (2016). Reliability of dissimilarity measures for multi-voxel pattern analysis. *NeuroImage*, *137*, 188–200. https://doi.org/10.1016/j.neuroimage.2015.12.012

Wang, X., He, C., Peelen, M. V., Zhong, S., Gong, G., Caramazza, A., & Bi, Y. (2017). Domain selectivity in the parahippocampal gyrus is predicted by the same structural connectivity patterns in blind and sighted individuals. *The Journal of Neuroscience*, 3622–16. https://doi.org/10.1523/JNEUROSCI.3622-16.2017

Wang, X., Peelen, M. V, Han, Z., He, C., Caramazza, A., & Bi, Y. (2015). How Visual Is the Visual Cortex? Comparing Connectional and Functional Fingerprints between Congenitally Blind and Sighted Individuals. *The Journal of Neuroscience : The Official Journal of the Society for Neuroscience*, *35*(36), 12545–12559. https://doi.org/10.1523/JNEUROSCI.3914-14.2015

Watkins, K. E., Shakespeare, T. J., O'Donoghue, M. C., Alexander, I., Ragge, N., Cowey, A., & Bridge, H. (2013). Early Auditory Processing in Area V5/MT+ of the Congenitally Blind Brain. *Journal of Neuroscience*, *33*(46), 18242–18246. https://doi.org/10.1523/jneurosci.2546-13.2013

Weeks, R., Horwitz, B., Aziz-Sultan, a, Tian, B., Wessinger, C. M., Cohen, L. G., … Rauschecker, J. P. (2000). A positron emission tomographic study of auditory localization in the congenitally blind. *The Journal of Neuroscience : The Official Journal of the Society for Neuroscience*, *20*(7), 2664–2672. Retrieved from http://www.ncbi.nlm.nih.gov/pubmed/10729347

Wolbers, T., Klatzky, R. L., Loomis, J. M., Wutte, M. G., & Giudice, N. A. (2011). Report Modality-Independent Coding of Spatial Layout in the Human Brain. *Current Biology*, *21*(11), 984–989. https://doi.org/10.1016/j.cub.2011.04.038

Xue, S., Weng, X., He, S., & Li, D. (2013). Similarity representation of pattern-information fMRI. *Chinese Science Bulletin*, *58*(11), 1236–1242. https://doi.org/10.1007/s11434-013-5743-0

Zeng, H., & Constable, R. T. (2002). Image distortion correction in EPI: Comparison of field mapping with point spread function mapping. *Magnetic Resonance in Medicine*, *48*(1), 137–146. https://doi.org/10.1002/mrm.10200

Acknowledgement: We would like to express our gratitude to Marco Barilari, Stefania Benetti, Giorgia Bertonati, Francesca Barbero who have helped with the

data acquisition, to Yangwen Xu for giving comments on a preliminary version of the paper, to Jorge Jovicich for helping to set-up the fMRI acquisition parameters and to Pietro Chiesa for continuing support with stimuli-delivery systems. We are also extremely thankful to our blind participants and to the Unioni Ciechi of Trento, Mantova, Genova, Savona, Cuneo, Torino, Trieste and Milano and the blind Institute of Milano for helping with the recruitment. The project was funded by the ERC starting grant MADVIS (Project: 337573) and the Belgian Excellence of Science program (Project: 30991544) awarded to Olivier Collignon. Olivier Collignon is research associate at the Fond National de la Recherche Scientifique de Belgique (FRS-FNRS).

Author contributions: SM and OC designed the research; SM, KMC, CB, RB, MVA and OC performed the research; SM, MR, CB, MVA, NNO and OC analysed the data; SM and OC wrote the paper; MR, CB, KMC, MVA, RB and NNO gave feed-backs on a draft of the manuscript.